*The Second International Conference on Infrastructure Management, Assessment and Rehabilitation Techniques*
*ICIMART'16*
*March 8-10, 2016*

# FRP Retrofitting of Bridges

Keynote Lecture by
**Dr. Khaled Galal**
Professor
Department of Building, Civil and Environmental Engineering
Concordia University
Montréal, Québec, Canada

**Abstract:**

Deterioration of ageing bridges has been well noted worldwide. Retrofit of deteriorated infrastructure has become a major challenge for governments in developed countries in the last decades. In response, there has been an escalating world-wide tendency to select Fiber Reinforced Polymer (FRP) composite retrofit systems as an alternative to traditional bridge rehabilitation schemes. Accordingly, several design codes were developed to standardize the bridge strengthening process using FRP systems. This lecture reports on ongoing research program at Concordia University that aims at investigating the effectiveness of external FRP strengthening of bridge elements such as T-girders, inverted-T bent caps, column and wall piers. The presentation promotes the consideration of FRP for bridge retrofitting by overviewing the material and methodologies, comparing the requirements of current codes, reviewing the state of the art, and in due course, addressing the limitations and future challenges.

## Background

The deterioration of infrastructure has been a major concern for governments in developed countries for decades. Aging, exposure to harsh environments, corrosion of steel, higher traffic demands, changes in use, poor initial design, collision damage, deferred maintenance, overuse and construction errors are the main factors contributing to the deterioration of the bridges, leading to deficiencies such as inadequate flexural, shear and ductility capacities. Additionally, in Canada and the U.S, nearly 50% of the bridges are pre-code, and do not satisfy the stringent requirements of the current advanced design codes (Galal and Mofidi, 2009).

## Structural Strengthening

Due to the fact that the replacement of a deteriorated structure/member can be extremely costly and inconvenient, structural strengthening to either stop or delay the accelerated deterioration has been of paramount importance to the authorities. According to FHWA (2010), 21% of the bridges in the U.S require some form of retrofit, modification, or upgrade to remove the deficiencies and restore function. On the other hand, the emergence of seismic retrofit as a new challenge, particularly in areas with high seismicity, promoted the structural strengthening even further. For instance, since 1995 and after the Hyogoken-Nanbu earthquake in Japan, strengthening of bridges with the purpose of seismic retrofit has become at least equally important if not more important than strengthening for solely stopping the deterioration.

## Traditional Methods of Strengthening

Several traditional rehabilitation schemes have been proposed for RC structures. Having been in use since the mid-1960s, bonding steel plates to the external concrete surface is one of the most common strengthening procedures. However, the de-bonding of the steel plates due to the degradation of the bond together with the difficulties in implementation (e.g. need for scaffolding, limited delivery dimensions of the plates, being heavy to transport , etc.) often make this method unpleasant. RC members have also been rehabilitated using the external post-tensioning techniques. Similarly, this method has not always been favorable due to the limitations such as corrosion of pre-stressed cables, losses of pre-stress and of course space constraints. Another well-known scheme is jacketing using RC or steel jackets which has shortcomings such as increasing the dead load and the dimensions of the member and providing unnecessary increase in stiffness. Epoxy injection, cathodic protection and spot-patching are other traditional techniques for rehabilitation of RC members. As long as the strengthening of the steel structures is the matter of concern, bolting or welding steel plates has been in use for decades. This process has disadvantages such as increasing the dead load of the member, development of weld fatigue cracks in areas with stress concentration and requires extensive drilling and lap splice detailing. It is noteworthy that all the aforementioned rehabilitation techniques were often costly in a way that the authorities often had tendency towards deferring the rehabilitation process, and instead taking temporary measures such as imposing load restrictions on bridges. This had worsened the performance of bridges, and accelerated the deterioration process.

## Innovative Methods of Strengthening

Since the traditional methods of strengthening were often inefficient and costly, the need for introducing innovative materials and methodologies became much more needed. Fiber Reinforced Polymer (FRP) composites offer advantages such as high modulus of elasticity, lightness, corrosion resistance, high strength to density ratios, high fatigue strength, tailorable performance characteristics, adaptable electromagnetic properties, easy application in confined spaces and ease of installation. These composites were firstly introduced in the 1940s, however, due to their being costly, their initial application was limited to shipbuilding, aerospace and defense industries. Having recognized the huge benefits of the FRP material, researchers tried to reduce the cost of these composites so that they can be used in construction industry as well. Nowadays, thanks to the ongoing research and several demonstration projects, FRP strengthening has emerged as a viable alternative to traditional schemes for flexural, shear and confinement strengthening of RC and steel bridges (Other innovative methodologies such as shape memory alloys (SMA), are still progressing compared to FRP strengthening systems).

It is important to note that, in spite of all the efforts in reducing the cost of the FRP material, the initial cost of FRP material is often higher in comparison to traditional material. Nonetheless, this initial higher material cost is offset by reduced labor, use of machinery, and shut-down costs. Therefore, in most cases the FRP offers the most economical solution for bridge rehabilitation.

## FRP Material and Properties

FRP composite is the combination of the load-bearing, stiff and strong fibers (Glass, Carbon, and Aramid (Kevlar)), with low-cost and lightweight polymers, binding the fibers together and protecting them against environmental actions. The fibers and polymers can be combined in any improvised manner; however, this is prohibited because of the uncertainty of the short and long-

term performances (ACI, 2002). FRP material are linear elastic under tension and do not yield, hence, the redistribution of the moments is not allowed and seismic energy cannot be dissipated due to the lack of plasticity. In addition, composites are anisotropic and weak in the transverse direction. Among fibers, Glass is the most common one having the largest elongation, lowest cost and the best corrosion resistance. That being said, Carbon is the most ideal fiber where high-strength, high-stiffness, lightweight and high fatigue resistance are the matter of concern.

**EB FRP Strengthening**

Since the 1990s, variety of girders, slabs, shear walls, columns, trusses, etc. have been retrofitted using externally bonded FRP laminates with unidirectional or bi-directional fiber orientations. This process was first introduced in Switzerland by Meier in 1984 with the purpose of structural repair (Barton, 1997), and was followed by the efforts of Caltrans (The California Department of Transportation) in the U.S during the early 1990s for seismically upgrading the columns using GFRP laminates (Sika Corp., 2012). Suppliers such as Sika, Fyfe and QuakeWrap, Cytec, amongst many others, generally offer two types of material to be used for externally bonded FRP strengthening: 1) Prefabricated and pre-cured strips/laminates bonded to the concrete using an epoxy, 2) Cured in situ, dry sheets/fibers having no resin inside (prepreg type has a very small amount of resin inside) where the epoxy not only bonds the sheet to concrete surface but also impregnates it.

Whether the former or the latter type of FRP material is used, a strong bond is required to achieve the composite action and to prevent the de-bonding of the FRP laminate from the concrete surface which is often the main cause of the failure (Meier 1995, Buyukozturk and Hearing 1998). The quality of the bond depends on factors such as existing concrete's condition, surface preparation, soundness of application and the durability of the epoxy, while parameters affecting the strength of the bond are chemical activity, exposure to ultra-violet radiation, temperature and moisture (Karbhari and Howie, 1997). In addition, FRP wrapping should be performed in a continuous way (in areas of discontinuity, lap splice should be formed), that allows the fibers to be oriented in the direction of the design tensile forces. It is clear that by changing the fiber orientation in various directions, different structural deficiencies can be addressed and resolved.

**Codes for EB FRP Strengthening**

Having the shear, flexural and confinement strengthening in mind, several design standards/guidelines have been developed to standardize the application of external epoxy-bonded FRP. In order to select the appropriate guideline, criteria such as accuracy, ease of use and format compatibility must be considered. Some of the widely known codes are:

- *ACI 440.2R Guide for the Design and Construction of Externally Bonded FRP Systems for Strengthening Concrete Structures (2008)* is the most well-known code in the United States. ACI also published *ACI 562 Code Requirements for Evaluation, Repair and Rehabilitation of Concrete Buildings (2013)* which permits the FRP strengthening and refers to ACI 440 for design requirements.
- *CNR 2004 Guide for the Design and Construction of Externally Bonded FRP Systems for Strengthening Existing Structures – Materials, RC and PC structures, masonry structures*

by Italian National Research Council, Rome, Italy. The recent update of this code is not translated in English yet.

- *FIB Bulletin No. 14 externally bonded FRP reinforcement for RC structures (2001)* by Federation Internationale du Beton (FIB). The guidelines for the design of FRP are compatible with design format of the CEB-FIP Model Code and Eurocode 2. This code is often used in conjunction with *FIB Bulletin No. 35. Retrofitting of concrete structures by externally bonded FRPs, with emphasis on seismic applications (2006).*
- *ISIS Design Manual No. 4 (2008) FRP Rehabilitation of Reinforced Concrete Structures ,* by the Canadian Network of Centers of Excellence on Intelligent Sensing for Innovative Structures. ISIS also participates in several code committees and sponsors several international conferences.
- *JSCE, 2001, Recommendations for Upgrading of Concrete Structures with use of Continuous Fiber Sheets* by Japan Society of Civil Engineers, Tokyo, Japan. In addition to design guidelines for FRP strengthening, this code highlights the recovery of structural functionality and measures to mitigate dis-benefits by preventing spalling.
- *Technical Report 55 (TR55) Design Guidance for Strengthening Concrete Structures Using Fibre Composite Materials (2000),* by The Concrete Society (TCS) in United Kingdom. TR 55 should be used in conjunction with *TR 57 Strengthening Concrete Structures Using Fibre Composite Materials: Acceptance, Inspection and Monitoring.*
- *Guide Specifications for Design of Bonded FRP Systems for Repair and Strengthening of Concrete Bridge Elements (2012)* by AASHTO is focused on EB FRP strengthening of reinforced and pre-stressed highway bridges to supplement the *AASHTO LRFD Bridge Design Specifications.*
- Several reports have been issued by National Cooperative Highway Research Program (NCHRP) for design/construction of FRP systems. Notably, NCHRP Report 678, *Design of FRP Systems for Strengthening Concrete Girders in Shear* (Belarbi et al. 2011), NCHRP Report 655, *Recommended Guide Specification for the Design of Externally Bonded FRP Systems for Repair Strengthening of Concrete Bridge Elements* (Zureick et al. 2010), NCHRP Report 564, *Field Inspection of In-Service Bridge Decks* (Telang et al. 2006), NCHRP Report 514, *Bonded Repair and Retrofit of Concrete Structures Using FRP Composites* (Mirmiran et al. 2004)

The design methodology in various FRP strengthening codes is based on the limit state theory, however, in order to find the ultimate strength codes use different reduction factors. In an FRP-strengthened member the overall strength is attributable to 3 different materials (concrete, steel and FRP), hence, codes either apply individual reduction factors separately to each material, or combined reduction factors to the whole composite. Some codes (e.g. ACI) use a combination of individual and combined factors. Most of the design codes fail to address the losses of FRP durability and bond strength losses over time, and this will lead to unrealistic reduction factors. Hence, the development of realistic reduction factors considering the long-time exposure of FRP to the environmental and load conditions has been the topic of many research papers.

Also, to ensure that the strengthened member will be able to carry the service loads and maintain a sufficient safety factor in the exceptional conditions where losses of strengthening occurs (e.g. fire, vandalism, severe corrosion, etc.), codes often set strengthening limits. The Table below

represents the limits in 6 widespread codes for external FRP retrofitting. Only the members respecting these limits will qualify for FRP strengthening.

Table 1: Strengthening Limits in Codes

| | |
|---|---|
| **AASHTO (2012)** | $f_c' < 8$ ksi<br>$R_r \geq \eta_i[(DC+ DW)+(LL + IM)]$ |
| **ISIS (2008)** | $(\phi R_n)_{existing} \geq (1.0 S_{DL} + 0.5 S_{LL})_{new}$<br>0.5 for LL is subject to increase |
| **ACI (2008)** | $(\phi R_n)_{existing} \geq (1.1 S_{DL} + 0.75 S_{LL})_{new}$<br>$(\phi R_n)_{existing} \geq (1.1 S_{DL} + 1.00 S_{LL})_{new}$<br>$(R_{n\theta})_{existing} \geq S_{DL}+S_{LL}$ |
| **CNR (2004)** | Factors to guarantee the durability are given |
| **JSCE (2001)** | No specific criterion or condition is given |
| **TR55 (2000)** | Logical engineering judgment is required |

**Flexural Strengthening**

In order to increase the flexural capacity and stiffness, reduce the distribution and width of the flexural cracks and improve the performance of the RC members under the service load conditions, the FRP material can be epoxy-bonded to the areas under tension while the fibers are oriented parallel to the principal stress direction. This type of strengthening can increase the ultimate flexural strength of the strengthened members from 10% to 160% (Meier and Kaiser, 1991; Ritchie et al, 1991; Sharif et al, 1994).

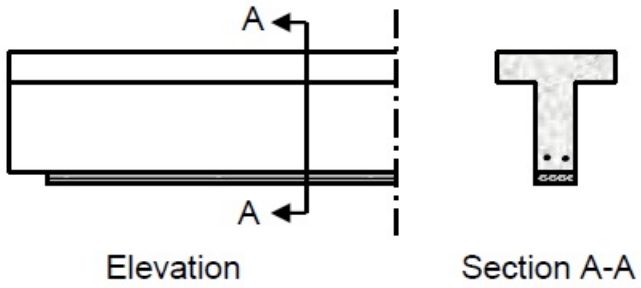


Figure 1: Typical Flexural Strengthening of a Reinforced Concrete T-beam Using EB FRP (ISIS Educational Module 4)

Variety of failure modes have been reported for members strengthened in flexure (CHBDC and ISIS): 1) Yielding of steel rebars followed by rupture of FRP; 2) Yielding of steel rebars followed by crushing of concrete in compression area (ductile) ; 3) Crushing of concrete in compression area before yielding of steel (brittle) ; 4) Shear failure of the concrete leading to FRP peel-off at the termination points (brittle) ; 5) FRP peel-off due to inclined shear cracks in the concrete; 6) FRP peel-off due to high tensile stresses in the adhesive (often ductile) ; 7) De-bonding at the FRP-concrete interface in areas of concrete surface unevenness (in. L-, or T-shapes, at the intersection

of web and flange due to minimal bonded length) or due to the lack of a solid bond. For the sake of simplicity, all these failure modes can be classified into two types (Thomsen et al. 2004) based on whether the composite action is maintained up to failure (1,2 and 3) or not (4,5,6 and 7). In order to avoid failure mode number 4, the codes oblige that:

Table 2: Limitations to Avoid End Peeling in Codes

| | |
|---|---|
| **AASHTO (2012)** | $f_{peel} \leq 0.065 \sqrt{f_c'}$<br>Otherwise, an anchorage system must be used |
| **ACI (2008)** | $If\ V_u > 0.67\ V_c$<br>An anchorage system must be introduced |
| **CNR (2004)** | $\tau_{be} \leq f_{b,d}$<br>Otherwise, an anchorage device must be used |
| **JSCE (2001)** | $\sigma_f \leq \sqrt{\frac{2G_f E_f}{n_f t_f}}$ |
| **TR55 (2000)** | Longitudinal shear stress between FRP and the substrate should not exceed 0.8 N/mm$^2$<br>&<br>At least 500 mm of anchorage length should be provided |

Although the failure mode number 2 is the most desirable (ductile), failure due to premature de-bonding due to propagation of an interfacial crack with residual shear stress acting along the interface was observed and identified by many researchers (Saadatmanesh and Ehsani 1989; Sharif et al. 1994). In fact, beams strengthened using the FRP epoxy bonding method are mostly susceptible to fail suddenly and without any precautions in a brittle manner due to de-bonding of the FRP sheet or laminate . Codes often set limits to FRP strain in a strengthened section to prevent de-bonding cracks from developing:

Table 3: FRP Strain Limitations in Codes for Members Strengthened in Flexure

| | |
|---|---|
| **AASHTO (2012)** | $\frac{\varepsilon_{frp}^{u}}{\varepsilon_{frp}^{y}} \geq 2.5$ |
| **ISIS (2008)** | $\varepsilon_{FRP} = 0.006$<br>Same as CSA-S806-02 (2002) |
| **ACI (2008)** | $\varepsilon_{fd} = 0.083 \sqrt{\frac{f_c'}{n E_f t_f}} \leq 0.9\ \varepsilon_{fu}$ (in.-lb. units)<br>$\varepsilon_{fd} = 0.41 \sqrt{\frac{f_c'}{n E_f t_f}} \leq 0.9\ \varepsilon_{fu}$ (SI units) |
| **CNR (2004)** | $\varepsilon_{fd} = min\ \{ \eta_a \frac{\varepsilon_{fk}}{\gamma_f}, \varepsilon_{fdd} \}$ |
| **JSCE (2001)** | No specific criterion or condition is given |
| **TR55 (2000)** | $\varepsilon_{frp} < 0.8\%$ for uniform load<br>$\varepsilon_{frp} < 0.6\%$ for combined shear and flexure |

In order to calculate the flexural capacity of a member strengthened using FRP material, it is assumed that the plane sections remain plain, the bond between concrete/steel and concrete/FRP is perfect, the contribution of tensile concrete to the flexural strength is negligible, initial strains in the section at the time of strengthening can be ignored and adequate anchorage and development length have been provided for FRP material (ACI and AASHTO). Additionally, TR55 assumes that the addition of FRP has nothing to do with the calculation of the location of the neutral axis, and instead, an additional capacity should be added to the capacity of the original section. The moment capacity of an FRP-reinforced section can be found as shown below:

Table 4: The Flexural Capacity in Codes

| | |
|---|---|
| **AASHTO (2012)** | $M_r = 0.9[A_s f_s (d_s - k_{2c}) + A'_s f'_s (k_{2c} - d'_s)] + \phi_{frp} T_{frp} (h - k_{2c})$ |
| **ISIS (2008)** | No specific design equations for flexure is given |
| **ACI (2008)** | $M_n = A_s f_s (d - \frac{\beta_1 C}{2}) + \psi_f A_f f_{fe} (h - \frac{\beta_1 C}{2})$ |
| **CNR (2004)** | No specific design equations for flexure is given |
| **JSCE (2001)** | No specific design equations for flexure is given |
| **TR55 (2000)** | $M_r = F_s z + F_f [z + (h - d)]$ |

As it can be seen in many codes the methodologies are similar to those used for regular RC sections with some modifications. The reduction factors for the calculation of flexural strength in different codes are summarized below:

Table 5: Flexural Strength Reduction Factors in Codes

| | |
|---|---|
| **AASHTO (2012)** | Fixed-value reduction factor of 0.85 for EB FRP |
| **ISIS (2008)** | A set of material resistance factors for various FRP schemes used in bridge strengthening are introduced |
| **ACI (2008)** | $\phi = \begin{cases} 0.90 \; for \; \varepsilon_t \geq 0.005 \\ 0.65 + \frac{0.25 (\varepsilon_t - \varepsilon_{sy})}{0.005 - \varepsilon_{sy}} \; for \; \varepsilon_{sy} < \varepsilon_t < 0.005 \\ 0.65 \; for \; \varepsilon_t \leq \varepsilon_{sy} \end{cases}$ FRP reduction factor $\psi_f = 0.85$ |
| **CNR (2004)** | Partial safety factors: $\gamma_{Rd}$ which depends on the resistance model; either bending, shear, or confinement. $\gamma_m$ which depends on mode of failure and application type. |
| **TR55 (2000)** | $\gamma_{mF} = \gamma_{mf} \cdot \gamma_{mm}$ |

**Shear Strengthening**

The shear strength of an RC beam is attributable to aggregate interlock, compressive zone concrete, dowel action, and transverse steel reinforcement, and can be increased significantly by bonding the

FRP composites externally to the RC member, having the fibers crossing the shear cracks and parallel to principal tension stresses. Thereby, the beam will fail in flexure and the brittle shear failure can be avoided. To this end, the FRP composite is bonded to the beam covering either only the two sides of the beam (side bonding), or the two sides together with the tension face (U-jacketing). It is noteworthy that, covering the whole cross-section (closed wrapping) is possible only in bridge columns (and not the girder), because of girder's being integral with the slab.

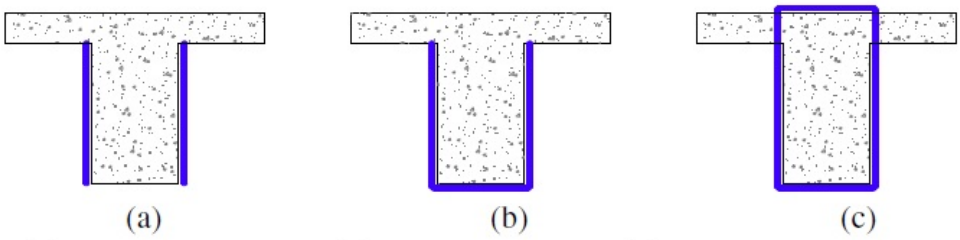


**(a) Side bonding, (b) U-wrap, and (c) Complete wrap**

Figure 2: Shear Strengthening Schemes (NCHRP Report 678)

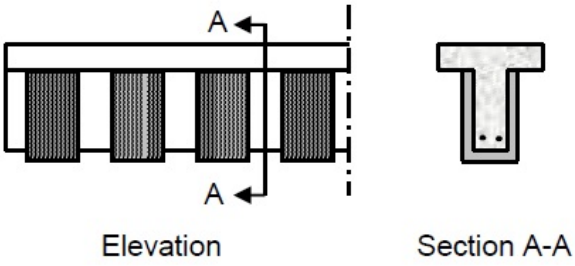


Figure 3: Typical Shear Strengthening of a Reinforced Concrete T-beam Using EB FRP (ISIS Educational Module 4)

The application of discrete FRP straps having the fibers oriented in 45 or 90 degrees to the longitudinal axis, is recommended by codes since it allows the migration of the trapped moisture (ACI and TR55). When discrete straps are used the strip spacing limitations must be respected.

Table 6: Spacing Limitations of Discrete Straps in Codes

| | |
|---|---|
| **AASHTO (2012)** | $if\ V_u < 0.125\ f_c'\ then\ S_{max} = 0.8\ d_v \leq 24\text{in}$<br>$if\ V_u > 0.125\ f_c'\ then\ S_{max} = 0.4\ d_v \leq 12\text{in}$ |
| **ISIS (2008)** | $S_{FRP} \leq W_{FRP} + d_{FRP}/4$<br>Based on CHBDC (CSA S6-06) |
| **ACI (2008)** | $S_{FRP} \leq W_{FRP} + d_{FRP}/4$<br>$if V_s + V_f \leq 4\sqrt{f_c'}\ b_w d$ use $S_{max} = \frac{d}{2} \leq 24\text{in}$<br>$if V_s + V_f > 4\sqrt{f_c'}\ b_w d$ use $S_{max} = \frac{d}{4} \leq 12\text{in}$ |
| **CNR (2004)** | $2\text{ in (50 mm)} \leq W_f \leq 10\text{ in (250 mm)}$<br>&<br>$W_f \leq \rho_f \leq \min\{0.5d, 3\ W_f, W_f + 8\text{ in (200 mm)}\}$ |

The failure mode depends on the geometry of the section, the wrapping scheme, the quality of the concrete substrate and the axial rigidity of the FRP, and may occur due to either de-bonding from sides (in bond-critical applications like side-wrapping and U-jacketing) or FRP rupture at stresses lower than ultimate FRP tensile strength (due to stress concentration at corners in closed-wrapping scheme). It is important to note that codes often limit the total shear reinforcement allowed as follows:

Table 7: Total Allowable Shear Reinforcement in Codes

| | |
|---|---|
| **AASHTO (2012)** | $V_n$ should not exceed $0.25 f_c' \ b_v \ d_v + V_p$ |
| **ISIS (2008)** | $V_c + V_s + V_{frp} \leq 0.25 \ \phi_c \ f_c' \ b_v \ d_v$ |
| **ACI (2008)** | $V_s + V_f \leq 8 \sqrt{f_c'} \ b_w \ d$ (in.-lb. units)<br>$V_s + V_f \leq 0.66 \sqrt{f_c'} \ b_w \ d$ (SI units) |
| **CNR (2004)** | $V_{Rd,max} = 0.3 \ f_{cd} bd$ |
| **TR55 (2000)** | Shear stress should be < $0.8\sqrt{f_{cu}}$ *or* 675 psi (5 N/mm$^2$) |

In addition to flexural capacity, codes provide equations to quantify the shear strength of a section strengthened using FRP sheets. To this end, it is assumed that FRP only carries normal stresses in the direction of principal fiber. Also, as mentioned before, the FRP material do not yield; hence, the actual strains in the FRP just before the shear failure of the concrete are important. This strain is referred to as the effective strain and is less than maximum tensile strain of the FRP. If the effective strain is multiplied by FRP's elastic modulus and the FRP cross sectional area, the result would be the shear strength provided by the FRP reinforcement which in turn depends on shear crack pattern and fiber orientation. The nominal shear strength and the contribution of the FRP sheet to shear strength in various FRP codes are as shown below:

Table 8: Nominal Shear Strength and FRP Contribution to Shear Capacity in Codes

| | | |
|---|---|---|
| **AASHTO (2012)** | $V_{frp} = \rho_f E_f \varepsilon_{fe} b_v \ d_f \ (sin \ \alpha_f + \ cos\alpha_f)$ | $V_n = V_c + V_s + V_{frp}$ |
| **ISIS (2008)** | $V_{FRP} = \frac{\phi \ frp \ Efrp \ \varepsilon_{frp} dfrp Afrp \ (cot\theta + \cot\beta) sin\beta}{Sfrp}$ | $V_r = V_c + V_s + V_{FRP}$ |
| **ACI (2008)** | $V_f = A_{fv} \ f_{fe} \ (sin\alpha + cos\alpha) \ d_{fv} \ / \ S_f$ | $V_n = V_c + V_s + \psi_f V_f$ |
| **CNR (2004)**<br>**U-Wrap:**<br><br>**4-sided Wrap:** | $V_{Rd,f} = \frac{1}{\gamma_{Rd}} \ min \ \{0.9d, \ h_w\} \ f_{fed} \ 2 \ t_f \ \frac{sin\beta}{sin\theta} \frac{W_f}{\rho_f}$<br>$V_{Rd,f} = \frac{1}{\gamma_{Rd}} \ 0.9 \ d \ f_{fed} \ 2 \ t_f \ (cot\theta + \cot\beta) \ \frac{W_f}{\rho_f}$ | $V_{Rd} = min\{ V_{Rd,ct} + V_{Rd,s} + V_{Rd,f}, V_{Rd,max}\}$ |
| **JSCE (2001)** | $V_{fd} = K[A_f \ f_{fud} \ (sin\alpha_f + cos\alpha_f) \ / \ S_f] \ Z \ / \ \gamma_b$ | $V_{fyd} = \ V_{cd} + V_{sd} + V_{fd}$ |
| **TR55 (2000)** | $V_{Rf} = (\frac{1}{\gamma_{mF}}) A_{fs} (E_{fd} \varepsilon_{fe}) sin\beta (1 + \cot\beta) (\frac{d_f}{S_f})$ | $= V_T = V_c + V_s + \ V_{Rf}$ |

Furthermore, FRP shear strength reduction factors are summarized in the table below in the different codes:

Table 9: Shear Strength Reduction Factors in Codes

| AASHTO (2012) | ISIS (2008) | ACI (2008) | CNR (2004) | JSCE (2001) | TR55 (2000) |
|---|---|---|---|---|---|
| 0.85 | 0.56 | 0.7 | 0.83 | 0.8 | 0.65 |

In order to prevent the formation of wide cracks leading to the loss of aggregate interlock (ACI), prevent de-bonding in 3-sided and 2-sided wrapping schemes (ACI and AASHTO), rupture failures in wrapping schemes where anchors have been used (AASHTO), and in order to respect the criteria such as: limits of FRP shear strengthening, limits of aggregate interlock and requirements in bond critical applications (ISIS), codes often limit the FRP design strain as follows:

Table 10: FRP Strain Limitations in Codes for Members Strengthened in Shear

| | | |
|---|---|---|
| **AASHTO (2012)** | 3-sided and 2-sided wraps | $\varepsilon_{fe}=R_f\varepsilon_{fu} \leq 0.004$<br>$R_f = 0.06 \leq 3(\rho_f E_f)^{-0.67} \leq 0.1$ |
| | Complete wrap | $\varepsilon_{fe}=R_f\varepsilon_{fu}$<br>$R_f = 0.088 \leq 4(\rho_f E_f)^{-0.67} \leq 0.1$ |
| **ISIS (2008)** | All wrapping schemes | $\varepsilon_{FRPe} \leq 0.75\varepsilon_{FRPu}$<br>$\varepsilon_{FRPe} \leq 0.004$ |
| **ACI (2008)** | 3-sided and 2-sided wraps | $\varepsilon_{fe} = K_v\,\varepsilon_{fu} \leq 0.004$ |
| | Complete wrap | $\varepsilon_{fe} = 0.004 \leq 0.75\varepsilon_{fu}$ |
| **CNR (2004)** | 3-sided and 2-sided wraps | 0.004 |
| | Complete wrap | 0.005 |
| **TR55 (2000)** | 3-sided wrap | 0.004 |

**Confinement Strengthening**

In seismic zones and in order to increase the ductility in the plastic hinges and prevent the de-bonding of the rebars in lap splices, columns are confined by the FRP laminates having the fibers directed normal to the longitudinal axis. Column confinement limits the dilation tendency of the concrete after a certain amount of ductility is achieved, depending on the circumferential rigidity of the fibers and bond quality. The confining stress transmitted to the columns increases as the corner radii increase; hence, confinement strengthening is less effective in rectangular columns and most effective in elliptical and circular columns. It is important to note that, in areas with low seismicity, confinement strengthening might still be performed to increase the capacity of the bridge or for blast resistance purposes.

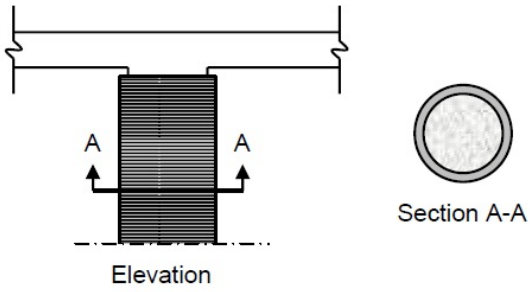


Figure 4: Typical Confinement (Axial) Strengthening of a Reinforced Concrete Column Using EB FRP (ISIS Educational Module 4)

Ideally, the failure of an RC column confined using FRP sheets should occur by fiber rupture, however, in many cases it occurs at strains lower than ultimate strain tested for tensile strength (Lorenzis, 2001). Reason being that as the hoop tensile strength of the concrete is reached, it expands laterally, and the axial strength provided by FRP wrapping will become obsolete. In order to avoid large deformations accompanied by crack propagation and spalling, codes limit the FRP strain as follows:

Table 11: FRP Strain Limitations in Codes for Confinement-Strengthened Members

| | |
|---|---|
| **AASHTO (2012)** | Maximum FRP strain in axial compression = 0.004<br>Maximum FRP strain in axial tension = 0.005<br>Maximum FRP strain in axial compression + bending = 0.003 |
| **ISIS (2008)** | Maximum confinement strain of 0.004 |
| **ACI (2008)** | $\varepsilon_{ccu} = \varepsilon_c' \ (1.50 + 12\ K_b \frac{fl}{f_c'} (\frac{\varepsilon_{fe}}{\varepsilon_c'})^{0.45})$<br>$\varepsilon_{ccu} \leq 0.01$ |
| **CNR (2004)** | FRP Strain < 0.4%<br>$\varepsilon_{fd,rid} = \min\{ \eta_a \frac{\varepsilon_{fk}}{\gamma_f}, 0.004\}$ |
| **TR55 (2000)** | Maximum FRP strain due to confinement = 0.010 |

Based on a stress–strain model used in different codes, the minimum and maximum confinement stress thresholds are presented below:

Table 12: Maximum and Minimum Thresholds of Confinement Stress in Codes

| | **Minimum** | **Maximum** |
|---|---|---|
| **AASHTO (2012)** | 600 psi | $f_l = \phi_{frp}\ 2N_{frp}/D \leq \frac{f_c'}{2}\ (1/k_e\ \phi - 1)$ |
| **ISIS (2008)** | $0.1\ f_c'$ | $0.33\ f_c'$ |
| **ACI (2008)** | $\frac{f_l}{f_c'} \geq 0.08$ | $f_{cc,u}' = f_c' + E_2\ \varepsilon_{ccu}$ |
| **CNR (2004)** | $If\ f_{l,eff}/f_{cd} > 0.05$<br>Confinement is effective | $f_{ccd} = f_{cd} + E_t\ \varepsilon_{ccu}$ |
| **TR55 (2000)** | N/A | $f_{ccd} = \frac{0.67 f_{cu}}{\gamma_{mc}} + 0.05(\frac{2\ t_f}{D})\ E_{fd}$ |

The increase in the column's load-bearing capacity due to FRP strengthening, depends on the strain in the FRP fabric which in turn is related to the lateral dilation of concrete. To calculate the gain in strength, codes replace the compressive strength of concrete $f'_c$, with $f'_{cc}$ which is the increased compressive strength of concrete. It is important to note that the increase in strength due to confinement will be realized only after lateral expansion of concrete due to the formation of cracks and yielding of rebars. The factored axial load resistance for a confined column and increased confined concrete compressive strength $f'_{cc}$ are taken as:

Table 13: Factored Axial Load Resistance and Increased Confined Concrete Compressive Strength in Codes

| | | |
|---|---|---|
| **AASHTO (2012)** | For spiral reinforcement members: $P_r = 0.85\phi[0.85f'_{cc}(A_g - A_{st}) + f_y A_{st}]$ For tie reinforcement members: $P_r = 0.80\phi[0.85f'_{cc}(A_g - A_{st}) + f_y A_{st}]$ | $f'_{cc} = f'_c(1 + \frac{2f_l}{f'_c})$ |
| **ACI (2008)** | Non-prestressed members with steel spiral reinforcement: $\phi P_n = 0.85\phi[0.85f'_{cc}(A_g - A_{st}) + f_y A_{st}]$ Non-prestressed members with steel tie reinforcement: $\phi P_n = 0.80\phi[0.85f'_{cc}(A_g - A_{st}) + f_y A_{st}]$ | $f'_{cc} = f'_c + \psi_f 3.3K_a f_l$ |
| **ISIS (2008)** | $P_r = 0.80[f'_{cc}\phi_c \alpha_1(A_g - A_s) + f_y \phi_s A_{st}]$ | $f'_{cc} = f'_c + 2f_{IFRP}$ |
| **CNR (2004)** | $N_{Rcc,d} = \frac{1}{\gamma_{Rd}} A_c f_{ccd} + A_s f_{fyd}$ | $\frac{f_{ccd}}{f_{cd}} = 1 + 2.6(\frac{f_{1,eff}}{f_{cd}})^{2/3}$ |

It is also noteworthy that, different codes use different strength reduction factors as follows:

Table 14: Axial Load Resistance Reduction Factors in Codes

| AASHTO (2012) | ISIS (2008) | ACI (2008) | CNR (2004) | TR55 (2000) |
|---|---|---|---|---|
| Confinement: 0.65<br>Spiral: 0.75<br>Ties: 0.65 | Concrete: 0.75<br>Steel: 0.9<br>CFRP: 0.56 | Spiral: 0.75<br><br>Ties: 0.65 | FRP Reduction : 0.90 | Concrete: 0.67 |

**Fatigue, Creep and Development Length Considerations**

Codes often limit the difference between maximum and minimum stresses to guard against fatigue and this varies significantly in different codes. In addition, limits are applied on the FRP reinforcement strain to avoid creep rupture. In general, AASHTO provides the most comprehensive checks for creep rupture and fatigue. These limitations in various codes are presented below:

Table 15: Stress and Strain Limitations in Codes to Avoid Creep and Fatigue

| | | |
|---|---|---|
| **AASHTO (2012)** | $\varepsilon_c \leq 0.36\frac{f_c'}{E_c}$<br>$\varepsilon_s \leq 0.8\varepsilon_y$<br>$\varepsilon_{frp} \leq \eta\ \varepsilon_{frp}^{u}$<br>η = 0.8, 0.5, and 0.3 for CFRP, AFRP, and GFRP (only if experimental data is not available) | to avoid both fatigue and creep (cyclic fatigue stresses found to be very close to those obtained for static creep) |
| **ISIS (2008)** | Difference between maximum and minimum stresses in steel rebars ≤ *125MPa* | to cope with fatigue (CAN/CSA S6-06) |
| | maximum stress level = *0.35* $f_{FRPu}$ *for* AFRP<br>maximum stress level = *0.65* $f_{FRPu}$ *for* CFRP<br>maximum stress level = *0.25* $f_{FRPu}$ *for* GFRP | to avoid creep rupture |
| **ACI (2008)** | $f_{f,s} \leq 0.20\ f_{fu}$ for GFRP<br>$f_{f,s} \leq 0.30\ f_{fu}$ for AFRP<br>$f_{f,s} \leq 0.55\ f_{fu}$ for CFRP | stress limits of FRP reinforcement (sustained and cyclic service load) |
| **CNR (2004)** | Stress should be limited to $\eta_1$ of ultimate<br>$\eta_1$ = 0.5 for AFRP<br>$\eta_1$ = 0.8 for CFRP<br>$\eta_1$ = 0.3 for GFRP | to control creep and relaxation |
| | $\eta_1$ = 0.5 (for all types of FRP) | fatigue control |
| **JSCE (2001)** | $\sigma_f \leq \sqrt{\frac{2\ \mu\ G_f\ E_f}{n_f\ t_f}}$<br>$\mu = 0.7$ | fixed value for creep rupture and fatigue limit control |
| **TR55 (2000)** | Stress should be limited to 80% of ultimate for CFRP<br>Stress should be limited to 70% of ultimate for AFRP<br>Stress should be limited to 30% of ultimate for GFRP | to control fatigue |
| | Stress should be limited to 65% of ultimate for CFRP<br>Stress should be limited to 40% of ultimate for AFRP<br>Stress should be limited to 55% of ultimate for GFRP | to control creep |

The capacity of the bond between concrete substrate and FRP sheet is essential for the member retrofitted using external FRP material. Good bond may help FRP sheet to develop sufficient tension force at a necessary length in the region of maximum moment. The tension development length is given in codes as follows:

Table 16: Tension Development Length in Codes

| | | |
|---|---|---|
| **AASHTO (2012)** | $L_d \geq \frac{T_{frp}}{b_{frp}\,\tau\,int}$ | - |
| **ACI (2008)** | $l_{df} = \sqrt{\frac{nE_f\,t_f}{\sqrt{f_c'}}}$ (SI units) | anchorage length of FRP should exceed the value of $l_{df}$ |
| **ISIS (2008)** | $l_a = 0.5\sqrt{E_{FRP}\,t_{FRP}} \geq$ 11.81 in | Anchorage lengths greater than $l_a$ must be provided otherwise anchorage system must be used |
| **CNR (2004)** | $l_e = \sqrt{\frac{E_f\,t_f}{2\sqrt{f_{ctm}}}}$ | $l_e$ in mm. |
| **TR55 (2000)** | $l_{t,max} = 0.7\sqrt{\frac{E_{fd}\,t_f}{f_{ctm}}}$ <br> $f_{ctm} = 0.18\,(f_{cu})^{2/3}$ | above $l_{t,max}$ increase in the bond failure force is impossible |

**FRP Strengthening: State of the Art**

In order to promote the application of FRP as a strengthening scheme, and having the improvement in ductility and strength of the structural members in mind, variety of research programs and demonstration projects have been conducted around the world. In this section, the state of the art in FRP strengthening is presented.

Many research programs have been focused on flexural strengthening using FRP. For instance, Lane et al. (1997) reported that the increase in flexural strength due to the application of continuous unidirectional FRP plates (with the thickness of 1–2 mm) is equal to that of using 6mm-thick steel plates. Also, Borowicz (2002); Quattlebaum et al. (2005); Manos et al. (2007) showed that by choosing mechanically anchored FRP strengthening scheme over the traditional externally epoxy bonded method, the flexural performance and ductility of the strengthened members can be improved dramatically, but the gain in flexural strength was much higher in the latter scheme. Subsequently, Galal and Mofidi (2009) developed a hybrid FRP sheet / ductile anchorage system that increased both ductility and flexural strength of RC T-beams.

In the case of steel structures, Gillespie et al. (1996) conducted full scale experimental test on deteriorated bridge steel girders and reported that stiffness and load carrying capacity of the girders retrofitted using carbon fiber can be increase by 25% and 100% respectively in comparison to deteriorated and non-retrofitted ones. Furthermore, Liu et al. (2001) investigated the behavior of steel bridge girders strengthened with FRP composite laminated strips. They concluded that the stiffness and plastic load capacity of the deteriorated steel girders can be increased when the CFRP laminates are attached to the tension flange of the girder, and the ultimate flexural capacity was improved considerably by 30% as well (Patnaik et al., 2008). Although FRP strengthening of steel members have been promoted in many research studies, due to low modulus of elasticity in

comparison to steel, often large amounts of FRP material is required to enhance the serviceability of the steel members. In order to deal with this obstacle, Rizkalla et al. (2008) proposed the application of high modulus CFRP (HM CFRP) plates, where the main concern was the limited delivery lengths of HM CFRP plates, necessitating lap splicing to cover the long spans of steel bridges. It was concluded that if the plate ends are reverse tapered, the gain in the capacity of bonded splice joints would be higher than that achieved by using specially designed mechanical anchors.

In order to provide additional shear strength for weak RC beams, Al-Sulaimani et al. (1994) cast series of small-scale rectangular RC beams deficient in shear, and then retrofitted the beams using GFRP sheets. The full potential of FRP shear strengthening was not realized since most of the beams failed in flexure. Chajes et al. (1995) and Triantafillou (1998), faced the same problem testing damaged beam without stirrups. It is now well recognized that full scale tests with internal shear reinforcements should be performed. That being said, Khalifa et al. (1999) tested three specimens strengthened in shear by U-jacketing, one of which was anchored using NMS technique. Thanks to the NSM system, the de-bonding failure which is very common in U-jacketing scheme was avoided. Lees et al. (2002) used non-laminated pre-stressed CFRP straps as the external shear reinforcement of RC beams. This method of shear strengthening changed the typical brittle failure to a ductile failure and delayed the formation of shear cracks, hence reported to be very appealing.

To investigate the effectiveness of FRP in confinement strengthening of L-shaped concrete columns, Karantzikis et al. (2005) conducted an experiment. They reported that the increase in strength and deformability is limited regardless of the FRP thickness due to the premature de-bonding at corners. They concluded that this can be prevented by using one of the anchoring methods. Hall et al. (2002) used a specially designed steel link to improve the connection between an FRP strengthened shear wall and the footing. This hybrid system allowed the yield of steel link before the rupture of FRP, hence; increased the ductility and energy dissipation capacity of the shear wall dramatically. Similarly, Nagy-Gyorgy et al. (2005) reported that if specific anchorage systems are used to avoid de-bonding the ductility and capacity can be increased significantly.

With a view to increase the shear strength of damaged wall specimens, Antoniades et al. (2005) applied FRP strips anchored using steel plates and angles. In addition, GFRP fan-type anchors were used along the development length of strips. The shear capacity of the walls increased significantly and shear cracking was controlled. However, given the huge damage during the test, it was concluded that FRP strengthening of the damaged walls is not comparable to the case of undamaged one. The effect of pre-damage and pre-loading was further studied by Assih et al. (1997). It was reported that the gain in strength was equal in both damaged and undamaged beams. Equal strength increase was observed in a study by Maalej and Bonacci (1998) in beams with or without sustained loads. In separate but similar studies, Arduini and Nanni (1997) and Tan and Mathivoli (1999) concluded that although the applied pre-load had no effect on the gain in strength, it reduced the stiffness of the beam. Also, when the pre-load was between the service and ultimate load, the gain in strength increased.

The effectiveness of anchorage systems have been the subject of concern in many research programs. Blaschko and Zilch (1999) conducted tests on concrete beams strengthened using NMS technique. Test results showed that this anchoring scheme is more effective in enhancing flexural and shear capacity of reinforced concrete beams compared to epoxy bonded FRP scheme. Bank et

al. (2002), Borowicz, (2002) and Velázquez et al. (2002), conducted full-scale tests on full-scale bridge T-girders in order to investigate the effectiveness of mechanically fastened FRP strips. All the strengthened beams failed prior to compressive failure of concrete and showed increases of 10-20% in strength at yield and ultimate loads. Borowicz (2002), also reported that end-termination distance and shear span can severely affect the capacity and failure mode of the mechanically fastened FRP strengthened beams, while cyclic loading does not cause the delamination of FRP strip. Ceroni et al. (2007) investigated the effectiveness of eight end fixing configurations for RC T-girders strengthened using EB FRP scheme. The tested end fixings were steel/FRP plates glued/bolted, FRP bars or L-shaped fibers. In most cases failure was due to de-bonding , however, the superior performances was obtained (the fibers failed in tension) in the case of using CFRP/steel plates and NSM bars transverse to strengthening direction.

Nordin (2003) and Jung et al. (2007) attempted to prestress the FRP strips used in the NSM technique in order to exploit the merged advantages of the two systems, where the FRP reinforcement was placed inside the epoxy-filled groove and prestressed against an independent steel reaction frame. However, their proposed methods have proven to be non-practical for field applications. Having this barrier in mind, Gaafar and El-Hacha (2008) proposed a hybrid anchorage/prestress system to strengthen reinforced concrete beams with prestressed FRP strips. Two steel anchors were bonded to the ends of each FRP strip, one being fixed at dead end and the other being free to move at jacking end and fixed to concrete using bolts after the termination of prestressing process. In fact, in the new proposed technique the FRP strip was prestressed against the beam itself. The results of the tests on 5 full scale RC beams showed that this method eliminates the premature de-bonding failure, improves the behavior at service load conditions and reduces the crack sizes.

Some research programs have focused on the development of analytical and numerical models for prediction of the behavior of FRP strengthened members. Pesic and Pilakoutas (2003) proposed a FE model to address the concrete cover delamination and plate end failure of concrete beams strengthened using externally epoxy bonded FRP. In addition, Elarbi (2011) used ABAQUS to predict the deformation and failure of concrete beams strengthened using EB FRP. Independent elements and nonlinear time-dependent material properties were used to account for loss of durability. FRP rupture in undamaged beams and FRP delamination in damaged beams where predicted successfully using this model. Ghobarah and Galal (2004) proposed a model to study the effect of eight different axial load variation patterns on the response of laterally loaded RC columns where the behavior of the elements was verified using experimental results. It was concluded that the magnitude of the axial load has a considerable effect on the lateral moment capacity of RC columns and that increasing the frequency of the axial load cycles will considerably decrease lateral moment capacity.

It is also worthwhile to mention that durability and long-term exposure of FRP to service and environmental conditions, and the consequent losses, have been investigated in many research programs. Karbhari (2004) reported that compared to below-freezing temperatures, the low temperature thermal cycling can be more deteriorative. In a more comprehensive study, Wu et al. (2006) investigated the effect of low temperature thermal cycling, cycling frequency, sustained loads, and salinity on FRP strengthened members. High-humid environment and sustained loads where the most overwhelming causes of the deterioration and can degrade the bond dramatically (Elarbi and Wu, 2012)

## Innovative Techniques and Anchorage Systems

As mentioned before, the most common type of failure for the beams strengthened in flexure is the de-bonding of the FRP material from concrete substrate which is categorized as a brittle failure. However, there are variety of anchorage systems that can be used to cope with this problem. As an example, transverse clamping by FRP U-wraps can increase the de-bonding strain by up to 30% (CECS- 146, 2003). Similarly, several anchorage systems have been proposed to solve the problem of de-bonding in 2-sided and 3-sided wrapping schemes used for shear strengthening, where due to high shear loads the FRP laminate detaches from the sides of the beam and premature brittle failure occurs. Furthermore, providing specially designed anchors reduces the chances of bulging due to excessive cracking and poor distribution of confinement stress in lateral load resisting confined columns (Ghobarah and Said, 2002; Ghobarah and Galal, 2004). With that being said, the importance of applying innovative techniques and anchorage systems to improve the behavior and failure mechanism of a strengthened member (in spite of the subsequent cost additions and installation complexity) is well-noted in many research studies, few of which have been described in this section.

### 1. Prestressed Sheets/Strips

Bonding FRP externally to a beam can increase the load-carrying capacity only under the ultimate load conditions since the plies are applied when the beam is under full dead load and deformations already exist in the beam. Nonetheless, to engage the full tensile capacity of the fibers, tensile prestress can be introduced which can significantly improve the behavior of the beam under service load conditions. In fact, prestressing the strips results in a more efficient use of FRP material by combining the benefits of both prestress and externally bonded systems. Furthermore, this system delays the formation of new cracks, reduces the total width of existing cracks by closing some and thanks to its small long-term losses, is very useful in restoring losses in conventionally prestressed beams (Hollaway and Garden 1998). In spite of all the advantages, this method is often labor-intensive and requires mechanical anchorage at high shear zones at termination points, hence the benefits must be balanced against cost additions.

### 2. Prestressed Straps

The shear strength of a beam can be increased dramatically by using prestressed CFRP strap system as the external shear reinforcement. This system prevents the de-bonding failure associated with conventional shear strengthening using externally bonded FRP laminates. In addition, this system does not require to be anchored to the concrete, provides a more appealing appearance by using thin straps and mitigates the premature failure at corners due to stress concentrations (Winistorfer, 1999). In this rehabilitation scheme the high-strength carbon fiber tapes are wound around the pad elements, then the strap is formed by fusion bonding CFRP layers one after another to the layer furthest from the center, and then is stressed. The biggest obstacle in wide application of this method is the conflict in determination of appropriate strap spacing, the reduction of which results in more prestressing effort (more cost) and the increase of which results in more unconfined zones leading to premature failure.

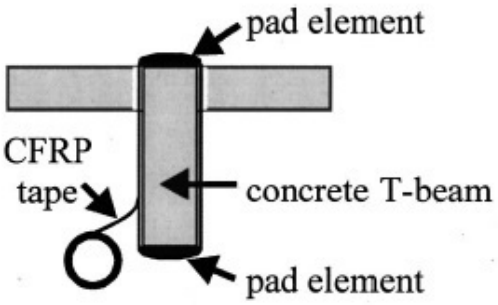


Figure 5: Application of Non-laminated Strap Elements (Lees et al., 2002)

### 3. Near Surface Mounted (NSM)

In this method, the FRP bars/sheets are placed in the narrow cuts on the surface of the member. Then, in order to transmit the force between the FRP sheet and concrete, the grooves are grouted (or filled by resin). This technique, can be tailored for shear/flexural strengthening of T-girders, walls, columns and slabs by positioning the slits at various locations. FRP bars can be placed before and after the corner for shear strengthening of beams or for flexural/ shear strengthening of walls and columns or at plane surface for flexural strengthening of beams and slabs. Additionally, this system offers advantages such as possibility of installation in curved and/or cracked substrates, being aesthetically appealing and not requiring extra protection. NSM technique increases the bonded area between the FRP and the concrete member; hence, higher capacities of FRP can be obtained compared to EB FRP method (El-Hacha and Rizkalla, 2004). The shortcomings of this method are increased efforts to drill the grooves and increase in the consumption of adhesive to fill the grooves. Also, in some cases due to small groove dimensions, de-bonding at the interface between FRP and the epoxy has been observed (known as epoxy-split failure)

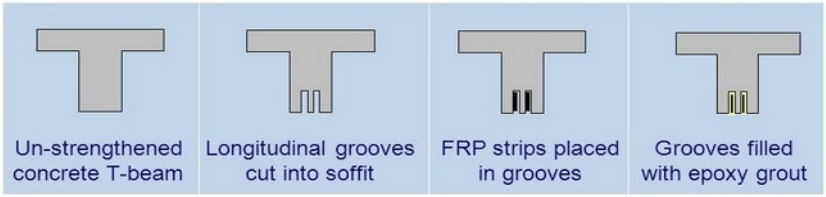


Figure 6: Near Surface Mounted FRP Strengthening Procedure (ISIS Educational Module 4)

### 4. Embedded Through-Section (ETS) FRP Rod Method

As mentioned before, both the NSM and EB FRP strengthening schemes require surface preparation and adhesive consumption, yet are susceptible to de-bonding (potential for de-bonding is higher in the latter scheme). Embedded Through-Section (ETS) technique has been proven to be less time consuming and needs lower amounts of adhesive. Also, since the surface preparation is not required, huge amounts of man-hours can be saved. However, the main advantage that makes this method of paramount importance is that unlike the aforementioned techniques; the FRP relies on the concrete core and not the surface. This provides more confinement which in turn improves the bond quality. To implement this

method, vertical holes are drilled through the middle of the cross section and the longitudinal axis of the RC beam. After removing debris by the means of water jet, one end of the hole is blocked using epoxy. Then ⅔rd of the adhesive volume required is poured into the hole while the remaining ⅓rd is applied around the CFRP rod. Finally, the rod is placed in the hole and the remainder of the adhesive is removed. In order to investigate the effectiveness of this method in increasing the shear capacity of the T-girders in comparison to NSM and EB FRP schemes, Chaallal et al. (2011) performed 12 tests on 6 full-scale RC T-beams retrofitted using various strengthening schemes (EB FRP, NSM and ETS). In addition, the effect of the presence of longitudinal and transverse steel rebars was investigated. It was concluded that, the average increase in shear capacity of the beam using ETS method was approximately 3 times greater than EB FRP method, and 2 times greater than NSM method. Also, the beams strengthened using EB FRP and NSM methods failed due to de-bonding and separation of the concrete side covers respectively. While using ETS technique, ductile flexural failure observed. That being said, important concerns such as the effects of the hole spacing, FRP rod type and cross-sectional area should be addressed by conducting further research.

## 5. Prefabricated Shapes

In order to avoid cuts all the way through the member (as in the case of NMS scheme) prefabricated angles (L-shaped profiles) can be externally bonded to the concrete surface in order to increase the shear capacity of the member. This method is easy to install and overcoat due to adjustable leg lengths and low thickness, respectively. It is important to note that overlapping the legs below the member forms a U-shaped profile similar to traditional shear reinforcement (stirrups).

Figure 7: L-Shaped Prefabricated FRP Profile (Sika Corp., 2014)

## 6. Mechanically Fastened FRP

Nailing the FRP at the desirable positions by the means of powder-actuated fasteners which install mechanical fasteners such as anchor bolts in the holes predrilled on the concrete surface is one of the most common anchorage systems. The problem of improper surface preparation leading to bubbling of the FRP and de-bonding failure associated with externally epoxy bonded FRP sheets are no longer a concern using mechanically fastened systems and the need of adhesive application and surface contamination removal can be eliminated as well. Moreover, using this technique, the waiting time for epoxy to be cured

(minimum 24 hours) can be eliminated (Sika Corp., 1999). However, shortcomings such as extensive cracking due to drilling holes, stress concentration and the consequent de-bonding at discrete drilled locations and corrosion of steel bolts often dictate the meticulous quantification of the benefits of this system and highlight the importance of ongoing research to find possible solutions.

## 7. Fan-type Anchorage

When enough anchorage cannot be provided by the means of full wraps or mechanical fasteners (e.g. at the internal corners of L-shaped or T-shaped sections), fan-type anchors are very efficient in providing sufficient anchorage capacity in shear strengthening of T-girders or confinement strengthening of columns. At the bottom side of the fan-type anchor, the fibers are dispersed while at the summit, the fibers are braided to form a tow. The tow part of the anchor is then placed in pre-drilled resin-filled holes in the concrete, while the dispersed part is spread outwards onto the FRP laminate anchoring of which is the matter of concern, and then are bonded to it using resin. Depending on the spacing of the anchors, the strength and ductility of the strengthened member can be increased effectively.

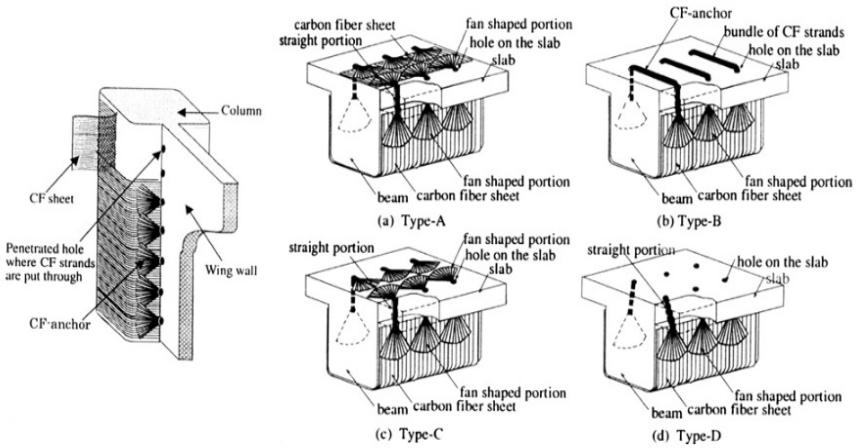


Figure 8: Fan-type Anchorage for Confinement (left) and Shear (Right) Strengthening (Koayshi et al., 2001)

## 8. Transverse Clamping using U-wraps

Transverse clamping using U-shaped fiber strips is one of the most traditional anchorage systems which not only prevents the premature failure due to de-bonding of the FRP laminate in the beams strengthened in flexure but also increases the strength and ductility. As mentioned before, transverse clamping by FRP U-wraps can increase the de-bonding strain by up to 30% (CECS- 146, 2003). It is noteworthy that if the U-wraps are concentrated at the termination points instead of being distributed along the beam, the beam would be susceptible to local slip and de-bonding with the loss of effectiveness.

**FRP Strengthening of Bridges**

Among all the structures retrofitted in shear/flexure using externally bonded composite fabrics, the bridges are of paramount importance since the traditional methods of repair are inefficient, and section enlargement/span shortening are often out of the question due to their being extremely costly. The first bridge successfully retrofitted using FRP material was the Ibach Bridge in Switzerland (Meier, 1992) and since then thousands of bridges have been retrofitted utilizing FRP material (Bakis et al 2002). With that being said, several factors should be considered before selecting FRP as the strengthening scheme for a bridge. First, the current condition of the bridge should be assessed by identifying the performance level and the extent and location of deficiencies. To this end, field investigations must be performed and data regarding the previous rehabilitations must be gathered. Then, the information regarding material properties, cracks, corrosion of rebars, dimensions, damaged members and required capacity to be achieved must be collected and finally the feasibility of FRP strengthening must be evaluated by not only considering mechanical performance, but also constructability, durability, and availability of the material.

Although the variety of bridge systems have been successfully retrofitted using different FRP strengthening schemes (mostly cast-in-place T-beam, precast I-girder and cast-in-place multi-cell box girder bridge systems) the main focus in this paper is given to slab on girder bridges (popular structural system of many existing bridges). This bridge system consists of a slab transferring loads transversely to longitudinal T-girders and an inverted-T bent cap that supports the longitudinal T-girders and transfers loads to piers and eventually bridge footing, hence, the ongoing research program at Concordia University that aims at investigating the effectiveness of external FRP strengthening of bridge elements such as T-girders, inverted-T bent caps, column and wall piers will be reported later on in this lecture.

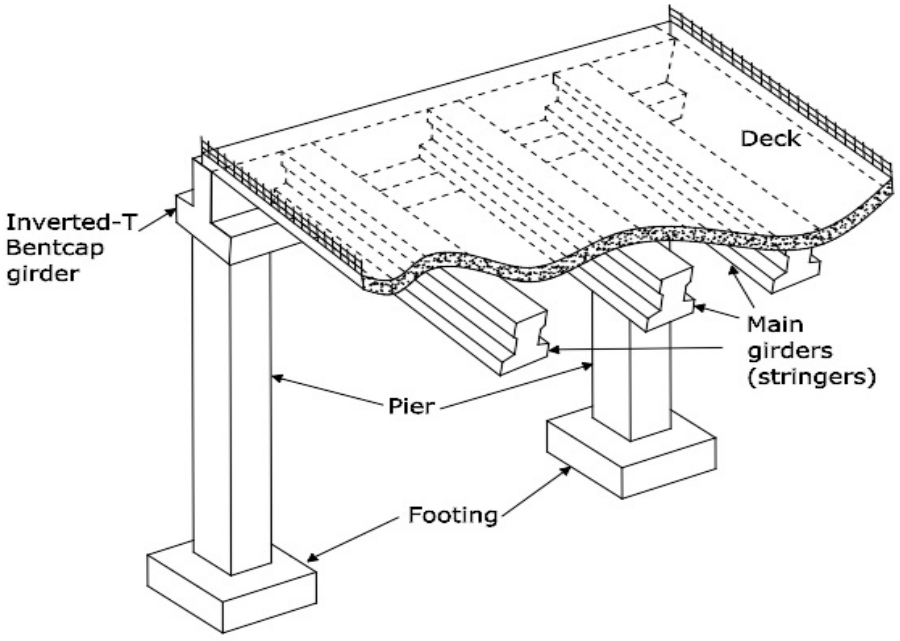


Figure 9: Slab on Girder Bridge

**T-girders Strengthened in Flexure Using New Mechanically Anchored System**

In order to increase RC T-girders' flexural strength and displacement ductility, a new mechanically anchored system which is composed of an FRP sheet(s) that could be bonded (or not) to the soffit of the RC beam is proposed. The FRP sheets are wrapped around two steel plates (160×40×13 mm) at theirs ends and then epoxy bonded (through an overlap) to the original FRP sheet. The overlap is to avoid de-bonding between the FRP sheets. The steel plate is then linked to an angle (64×64×13 mm) that is anchored to the beam support corner, through two steel link members and high tensile threaded steel rods (3/8"). The steel link members always have axial tensile forces (no moments) in them, and have a yield stress that is less than the ultimate strength of the total FRP sheets, hence yield before FRP ruptures. Consequently, the risk of peel-off and de-bonding of FRP sheets can be eliminated. In the case when FRP is un-bonded to the soffit of the beam only wrapping the FRP around the anchors is required. Here, the FRP sheet becomes into effect as the beam deforms and transfers the stresses to the end anchors and to the column stubs through the Hilti (HSL-3 M 24/60) anchors.

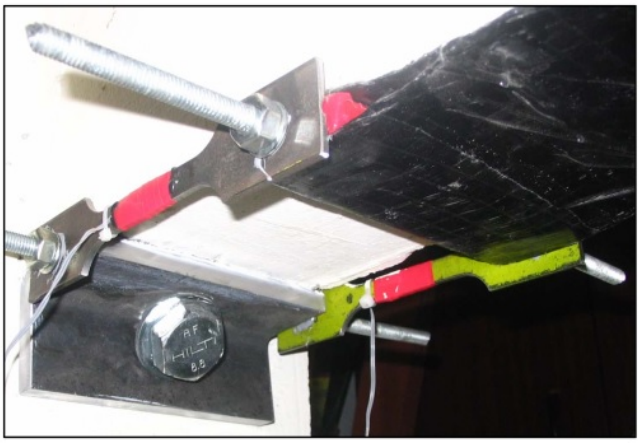

Figure 10: Ductile Anchor used in F-M-U & F-M-B (Galal and Mofidi, 2009)

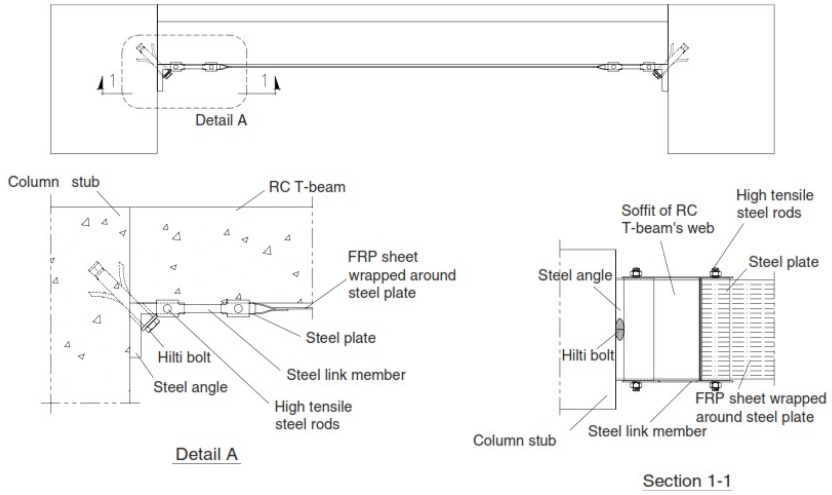


Figure 11: Proposed Hybrid FRP/Ductile Steel Anchor System (Galal and Mofidi, 2009)

In order to test the proposed system, four half-scale under-reinforced RC T-girders with two column stubs were cast. The details regarding supports, length of the girders, flexural reinforcement, flange reinforcement, the stirrups and reinforcement of column stubs are shown in the figure below. It is noteworthy that, the beams were overdesigned in shear to avoid a brittle shear failure. All four beams were tested under increasing monotonic four-point loading up to failure, or after reaching the end of the stroke of the actuator. The strains in longitudinal reinforcement, CFRP sheet, and steel links were monitored and deflections were measured at the

mid-span, loading points and the midpoint of the shear span. The crack opening and propagation were checked by visual inspection.

Beam F-C-O was tested as a control beam (not strengthened) while beam F-E-B was strengthened with conventional epoxy-bonded FRP. Beam F-M-U was strengthened with the new un-bonded hybrid FRP sheet/ductile anchor system and beam F-M-B was similar to F-M-U, yet the FRP sheet was bonded to the soffit of the beam by epoxy. All the retrofitted beams strengthened using 1 layer of FRP.

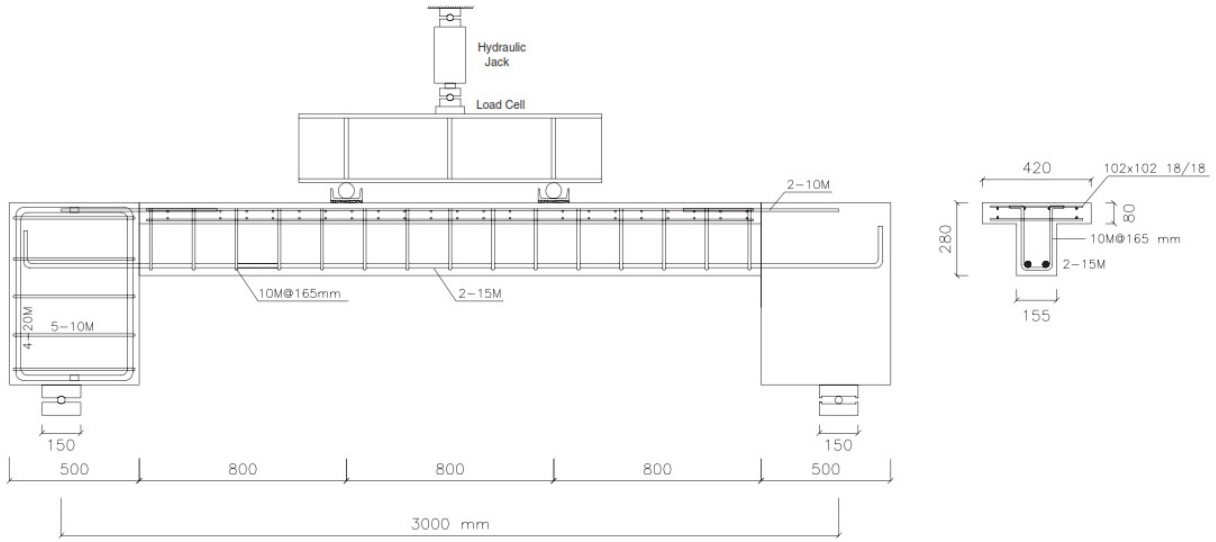


Figure 12: Dimensions and Details of Reinforcement of the Four Tested Beams (Galal and Mofidi, 2009)

The beam F-C-O failed by yielding of the steel reinforcement followed by crushing of the concrete. Specimen F-E-B failed prematurely without warning by de-bonding of the CFRP sheet after yielding of the steel reinforcement and had only 7% higher load capacity compared to control beam. F-E-B beam's strengthening mechanism increased the yield and the ultimate loads by about 16% and 5%, respectively, relative to those of the F-C-O and the ultimate mid-span deflection was 54% less than that of the control beam.

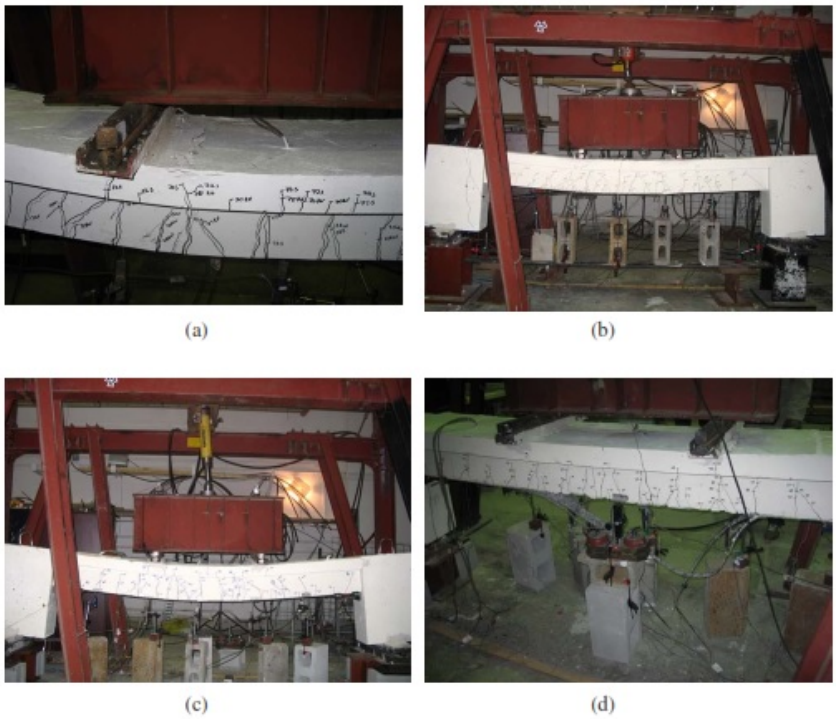


Figure 13: Tested Beams at Failure a) F-C-O b) F-E-B c) F-M-U d) F-M-B (Galal and Mofidi, 2009)

On the other hand, beam F-M-U resulted in about a 21% increase in the load carrying capacity compared to that of the F-C-O and showed a high displacement ductility level that reached 9.09, reason being the fully utilizing the capacity of the CFRP sheet through triggering yielding in the anchors, and allowing the beam to crack and deflect without being restrained by bond with the CFRP sheet. Finally, beam F-M-B showed an increase in the strength capacity of 27% compared to F-C-O, but failed due to the rupture of CFRP at a low displacement ductility of 3.37, mainly due to the high strains arising from being bonded at the locations of crack growths in the flexure zone. The presence of the hybrid FRP/ductile anchors prevented de-bonding of the CFRP sheet and eliminated the end peeling-off of the sheets; hence, the T-girder developed its full flexural capacity. The mid-span deflection at ultimate load was 19% lower than that of the control beam.

Consequently, it is safe to say that the best results were obtained by F-M-U beam (higher ductility, higher load capacity, no sudden de-bonding). Also, the mid-span deflection at maximum load of the F-M-U T-girder was about 366% higher than that of specimen F-E-B, 151% higher than that of specimen F-M-B, and even 96% higher than that of the control beam. It is worthwhile to note that, the differences between the predicted load capacities (using analytical guidelines of ISIS, ACI and FIB) and the experimental ones were within 10% for the four tested beams and within acceptable range.

**T-girders Strengthened in Shear Using New Mechanically Anchored System**

Most of the research efforts to study the retrofit of RC beams using FRP have been focused on flexural strengthening and among the few efforts directed towards shear strengthening, the attention has mostly been given to rectangular sections. Hence, in this research a new mechanically anchored system has been proposed to optimize the shear strengthening of T-girders using FRP composites. This system aims at using the full capacity of the dry fiber sheets, avoiding premature failures due to de-bonding, and maintaining ease of application.

To install the new system, firstly, the dry CF sheet is wrapped around two steel rods (25.4 mm diameter) and epoxy is applied only at the wrapped parts in order to prevent slip; secondly the corners of the soffit of the beam are chamfered to prevent stress concentration; then holes are drilled in the designed locations at the intersection of the web and flange as well as in the rod; and finally, the jacket is put at its proper location and the bolts (HSL-3 M10 Hilti) are tightened in the predrilled holes, ensuring that the fibers are stretched uniformly along the strengthened zone. The method relies on using the full mechanical contribution of the dry carbon fiber sheets, which will be activated upon development of strain in the RC web and initiation of shear cracks, and transferring them through a longitudinal steel rod to the core of the compression web-flange zone by the means of mechanical anchors. Instead of the dry CF sheet, mechanically anchored dry CF strips with specific spacing could be used. The diameter of the steel rod and the width of the strips can be designed such that the rod would not yield before rupture of the dry CF.

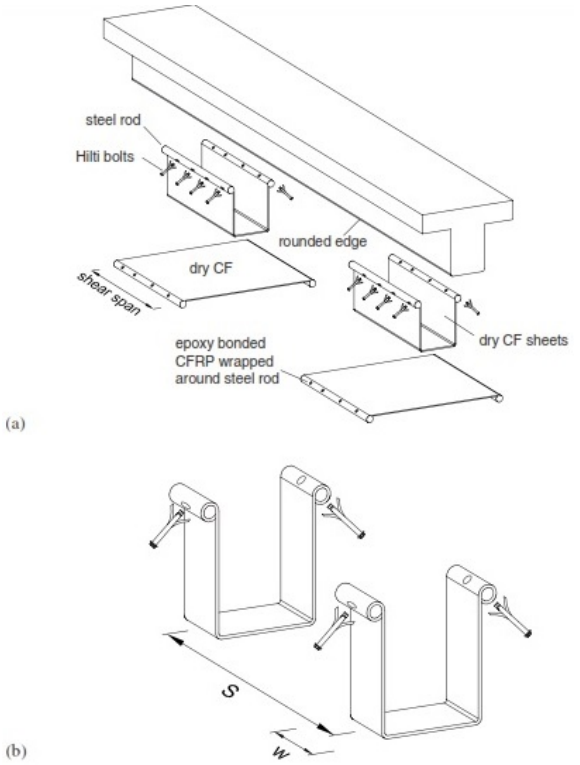


Figure 15: View of the Strengthened Beams (Galal and Mofidi, 2010)

Figure 14: Anchored U-shaped Dry CF Strips a) Continuous Sheet b) Strips of Width *w* with Spacing *S* (Galal and Mofidi, 2010)

In order to investigate the effectiveness of the proposed system, 3 half-scale RC T-beams were tested to failure: S-C-O (the concrete original beam); S-E-B (beam strengthened using epoxy bonding technique and single ply of FRP); and S-M-D (beam strengthened using the new system). The locations and the numbers of the anchors in beam S-M-D were highly overdesigned such that the rods not fail before the CF sheet reaches ultimate capacity. All three beams were tested under four-point loading up to failure. Details regarding the span length, shear span, flexural reinforcement and stirrups are shown in the figure below. Beams were designed to have flexural capacity that is approximately 1.7 times higher than the shear resistance, in order to guarantee a shear failure in the T-beam.

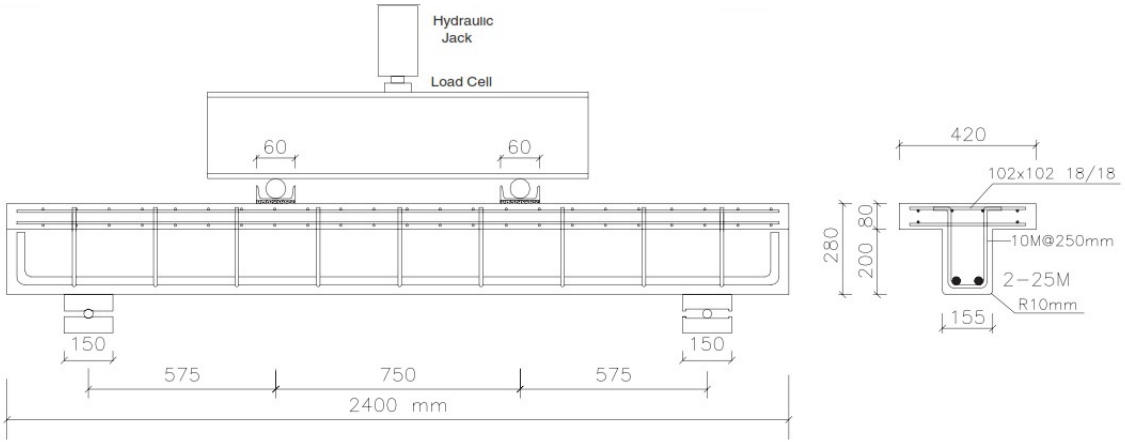


Figure 16: Dimensions and Details of Reinforcement of the Beams (Galal and Mofidi, 2010)

Upon loading beam S-C-O, diagonal shear cracks initiated at the middle of both shear spans concurrently at a load of 145 kN. As the load increased, the major crack extended upward through the flange toward the loading point leading to a brittle failure. In S-E-B beam, failure started by de-bonding of the CFRP sheets over the major shear crack in the same location observed in beam S-C-O; though, according to the strain compatibility between the flange and the web and when the concrete strut formed in the web, a secondary effect in the top flange was created. As the applied load increased, the bottom of the beam close to the support attempted to rotate, but the large, wide flange restrained the movement leading to horizontal tensile strains in the top part of the flange near the loading point. Finally, these strains reached the ultimate tensile strength of the concrete, a vertical crack was created on the top of the flange near the support, and then it spread descending towards web and CFRP. The bonded CFRP sheet eventually unzipped vertically. The load carrying capacity of beam S-E-B showed a 27% increase in the shear compared to S-C-O. In the beam S-M-D, the CF vertical fibers were able to bridge the diagonal shear cracks. As such, the abrupt de-bonding of the CFRP Sheet successfully prevented. Failure of the beam S-M-D occurred due to the formation of a major shear crack in the concrete beam. There was an increase in the shear capacity of 48% compared to the control beam S-C-O (and 27% compared to S-E-B) and 16% higher ultimate failure load over the CFRP bonded specimen S-E-B. Although the beam S-M-D was meant to fail in shear, yet the flexural steel started yielding and gained some ductility before the failure**.** It is anticipated that the contribution of the new U-shaped dry CFRP sheet strengthening system would have been higher if the beam S-M-D did not yield in flexure.

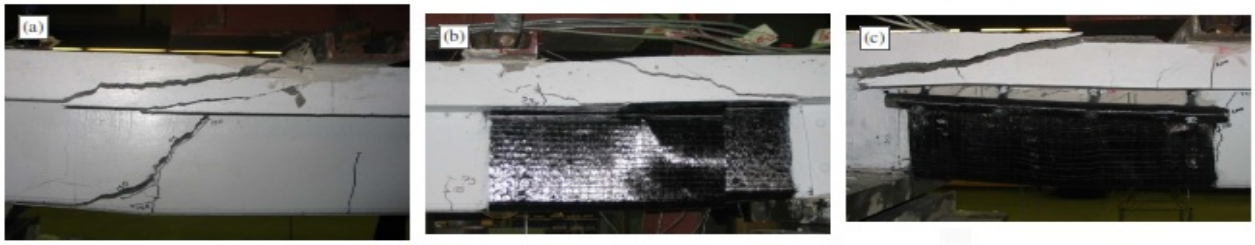


Figure 17: Cracking and Failure Pattern of Beams: a) S-C-O b) S-E-B c) S-M-D (Galal and Mofidi, 2010)

Comparing the mid-span deflection, beam S-M-D's deflection at the maximum load was 1.21 times the deflection of the beam S-E-B at the maximum load, whereas the beam S-C-O had the smallest deflection at the maximum load. In addition, comparison of vertical strain in the CF sheets in the beams S-M-D and S-E-B, showed that there were strains developing in the FRP in beam S-M-D slightly after the beginning of loading. Therefore, it could be said that the system starts contributing at service stage. In fact rapid increase in strain in CF in beam S-E-B shows that the CF was not involved in the initial stages of the loading. In addition, it is safe to say that higher strains in S-M-D indicate the maximum utilization of the strengthening sheet before the failure.

To get analytical results design guidelines of CSA A23.3 and CSA S6-06 were followed. The degree of correlation between the predicted and experimental results is calculated as a ratio of predicted values to experimental values. The shear strength analytical values were higher than the experimental failure loads up to 17% for the three tested beams. $V_{Analytical}$ for beam S-M-D showed the best correlation with the shear capacity reached during the test (6%). It is also noteworthy that**,** the experimental shear strength of T-beam S-M-D observed to be more than the shear strength of

a virtual T-beam with the same size and shape that is design adequately in shear based on shear reinforcement limits of Canadian code CSA A23.3. Also, a rough cost estimation on the two strengthening methods used in this research reveals that, although mechanically anchored method is cost saving regarding the time and labor needed for the surface preparation of the concrete, the two methods are approximately similar economically. All in all, while supplementary validation tests need to be conducted to completely understand the performance of RC beams strengthened with the proposed system, there are promising evidences that the new hybrid mechanically anchored dry CF U-jacket can make the FRP strengthening more attractive yet potentially economical for the retrofit of concrete structures.

**Steel Beams Strengthened in Flexure**

FRP material can be used for retrofitting of the steel structures as well. This offers advantages such as low-weight, ease of installation and also is very useful in covering areas with high bolt/rivet congestion. The biggest shortcoming of such technique is galvanic corrosion which can be stopped or slowed down by separating FRP from steel surface using an adhesive layer. Alternatively, small amount of glass beads can be mixed into 1mm of adhesive to prevent the galvanic corrosion. The main cause of failure in FRP-retrofitted structures is the premature de-bonding of FRP. Hence, an experimental study was conducted aiming at evaluation of the effectiveness of FRP systems in enhancing the flexural performance of deteriorated steel beams and investigating the functionality of a new anchorage system in prevention of de-bonding.

To this end, 13 medium-scale steel beams (W150×30) where tested in four-point bending. The artificial deterioration was achieved by area loss in the bottom flange to pretend the corrosion which negatively affects the flexural capacity. In fact, two different damage levels of 33% and 50% area reduction of the tension flange were considered in this study where the loss in area achieved either by the longitudinal notches located in the mid-span zone to simulate uniformly distributed corrosion, or holes that are localized at the mid-span section to simulate a local deterioration due to corrosion. The test matrix is shown below.

Table 17: Test Matrix (Galal et al., 2012)

| Group | Beams | ID | Area losses $mm^2$ | Retrofit material CFRP | Epoxy material | Retrofit method |
|---|---|---|---|---|---|---|
| G1 | B1 | BFO | None | — | — | — |
| | B2 | BF-H0.33 | 8 – 6.35 mm dia. holes | — | — | — |
| | B3 | BF-N0.33 | 2 – (25.4 × 450) $mm^2$ Notch | — | — | — |
| | B4 | BF-N0.50 | 2 – (38.1 × 450) $mm^2$ Notch | — | — | — |
| G2 | B5 | BF-H0.33-F1(5)-B1 | 8 – 6.35 mm dia. holes | SCH-11UP (5 layers) | Tyfo S | Fully bonded |
| | B6 | BF-N0.50-F1(5)-B1 | 2 – (38.1 × 450) $mm^2$ Notch | SCH-11UP (5 layers) | Tyfo S | Fully bonded |
| | B7 | BF-H0.33-F1(5)-B2 | 8 – 6.35 mm dia. holes | SCH-11UP (5 layers) | MB-3 | Fully bonded |
| | B8 | BF-N0.50-F1(5)-B2 | 2 – (38.1 × 450) $mm^2$ Notch | SCH-11UP (5 layers) | MB-3 | Fully bonded |
| G3 | B9 | BF-H0.33-F2(1)-B2 | 8 – 6.35 mm dia. holes | UC strip (1strip 1.4 mm) | MB-3 | Fully bonded |
| | B10 | BF-H0.33-F2(1)-B2w | 8 – 6.35 mm dia. holes | UC strip (1strip 1.4 mm) | MB-3 | Fully bonded |
| G4 | B11 | BF-H0.33-F1(1)-A1D1 | 8 – 6.35 mm dia. holes | SCH-11UP (1 layers) | — | Ductile anchorage |
| | B12 | BF-H0.33-F1(1)-A2D1 | 8 – 6.35 mm dia. holes | SCH-11UP (1 layers) | — | Ductile anchorage |
| | B13 | BF-H0.33-F1(5)-A1D2 | 8 – 6.35 mm dia. holes | SCH-11UP (5 layers) | — | Ductile anchorage |

All the beams in G2 retrofitted using FRP sheets bonded to the tension flange either using a saturating epoxy in a conventional wet-layup system or using a viscous epoxy, while the beams in G3 were rehabilitated using FRP plates externally bonded to the bottom flange either using viscous

epoxy or by wrapping a layer of CFRP sheet around the longitudinal CFRP plate and the bottom flange at both ends of the beam. The main purpose of testing G3 beams was the evaluation of the system in delaying de-bonding and increasing flexural strength.

Finally, the G4 beams were strengthened using innovative hybrid system of CFRP sheets/ductile anchorage in order to utilize a higher level of strain of the CFRP sheets by avoiding premature de-bonding through transferring the tensile stresses developed upon deformation of the loaded beam to the two ductile anchorage systems, and hence increasing flexural performance of CFRP retrofitted steel beams. The proposed retrofitting scheme consists of an un-bonded CFRP sheet that is attached to ductile anchorage systems, one at each end of the beam. The ductile anchor system consists of three parts. The CFRP sheets that are wrapped around Part 1 are connected to Part 3, which is rigidly attached to the steel beam by means of ductile link members designated as Part 2. Among 3 beams in G4, two were retrofitted using one layer of CFRP sheet that is wrapped around Part 1 of the anchorage system. One beam was designed such that the yield stress of the steel link is less than the tensile strength of the CFRP sheet used while in the other one the criteria was reversed. Also, in the third beam five layers of the CFRP sheets were wrapped around Part 1 of the anchorage system, also this beam had higher capacity than the CFRP sheet to have rupture in the CFRP sheet before yielding of the steel link.

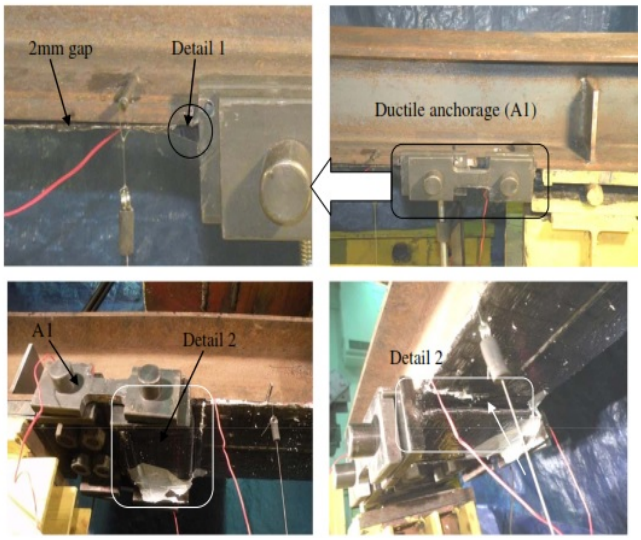


Figure 18: Ductile Anchorage with Detail 1 used in BF-H0.33-F1(1)-A1D1 & BF-H0.33-F1(1)-A2D1, with Detail 2 used in BF-H0.33-F1(5)-A1D2 (Galal et al., 2012)

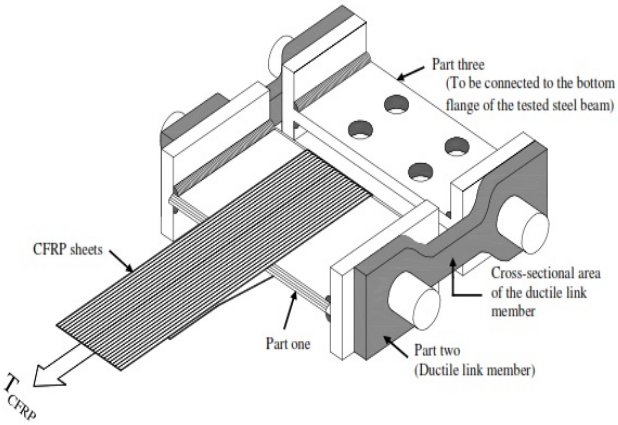


Figure 19: Details of the Ductile Anchorage (Galal et al., 2012)

Comparing the load-deflection curves of all beams one should acknowledge that, the beams with distributed deterioration (notches) showed lower stiffness than those with local deterioration (holes), yet the load causing first yield was equal in both deteriorated beams of course if the level of deterioration is same in both types. The non-linear transition towards plastic behavior was found to be steeper in locally deteriorated beams compared to those with spread deterioration. The non-deteriorated beam's yield load is exactly equal to the load at first yielding; hence, the beams do not show a clear yield plateau and to define the point of yield, arbitrary proof strain of 0.002 of the displacement at the first measured yield strain in the original section of the beam was defined.

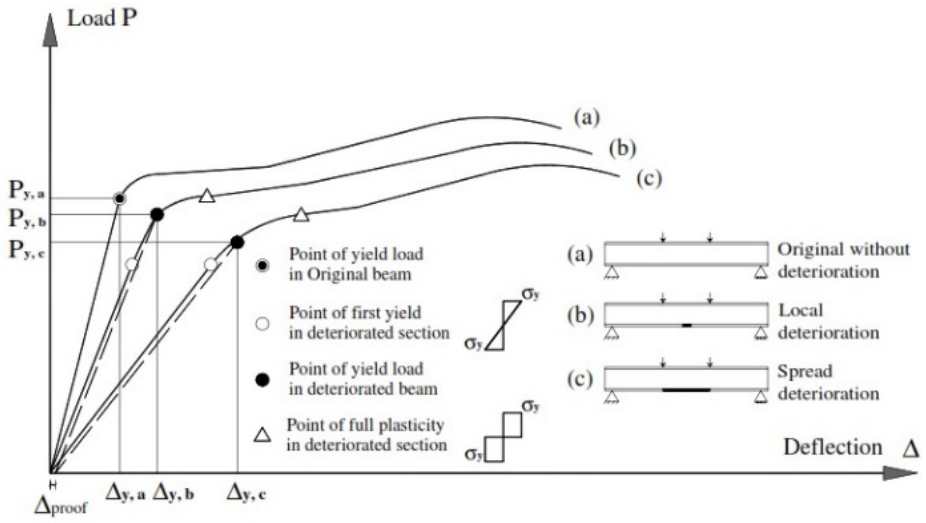


Figure 20: Load-deflection Relationship of Simply Supported Steel Beams: (a) No Deterioration; (b) Local Deterioration in the Mid-span Section; (c) Spread Deterioration in the Mid-span Zone (Galal et al., 2012)

In group G1, the difference between the load-deformation performance of the locally deteriorated beam and the control beam was insignificant due to the insignificant reduction in the stiffness. However, a significant difference in their load-strain performance was observed reason being that beams with local corrosion will experience a local increase in strains in the corroded section. In addition, increasing the level of area loss in the bottom flange for beams with spread deterioration from 33% to 50%, resulted in a respective reduction in both load-deflection and load-strain performances of the beams compared with the original beam. In the beams of group G2, the load-deflection and load-strain relationships for the four retrofitted beams was linear until yielding of the steel, after which the beams experienced a nonlinear behavior until the failure of the CFRP sheets occurred by either rupture or de-bonding. The beams with spread deterioration (notches) showed more non-linearity compared to those with local deterioration (holes), that being said; after failure of CFRP, both types of deteriorated beams followed the behavior similar to their respective un-retrofitted ones. It is important to note that, the beams (whether deteriorated extensively or locally) retrofitted using CFRP bonded by viscous epoxy showed higher ultimate flexural capacity compared to those in which saturated epoxy was used to bond. Furthermore, the yield moment of all beams in G2 was higher than their respective beams in G1 due to post-yield stiffening effect of CFRP sheets; however, this resulted in reduced displacement ductility. In G3, using transverse CFRP wraps around the bottom flange at the ends of bonded CFRP retrofit system did not have significant influence on delaying the de-bonding of the CFRP plates and the failure occurred due to peeling of the CFRP plate at the plate ends. Finally in G4, the first two beams with one sheet of CFRP both failed according to their respective design criteria. The anchorage system did not experience a local failure, which implies that it is effective in this regard. In the third beam, increasing the number of CFRP sheets resulted in lower FRP strain when the steel link yielded, which resulted in higher ultimate deflection and the CFRP sheets started to strain and get engaged in increasing the flexure capacity of the retrofitted beams at an early load level. It is worthwhile to note that, the third beam that was originally designed to have a ductile failure by yielding of the steel link members experienced a premature failure in the connection between the CFRP sheets and

anchorage system. This highlights the importance of the detailing of the anchorage system and the means of transferring stresses in its components. The modes of failure together with loads and deflections at yield and failure are shown in the table below.

Table 18: Summary of Test Results (Galal et al., 2012)

| | | At yield | | At failure | | |
|---|---|---|---|---|---|---|
| Group | Beam ID | Load $P_y$ (kN) | Defl. $\Delta_y$ (mm) | Load $P_u$ (kN) | Defl. $\Delta_u$ (mm) | Mode of failure |
| G1 | BFO | 245 | 7.7 | 331 | 73.6 | Steel-buckling |
| | BF-H0.33 | 242 | 8.0 | 330 | 69.8 | Steel-buckling |
| | BF-N0.33 | 190 | 6.4 | 311 | 74.3 | Steel-buckling |
| | BF-N0.50 | 155 | 5.8 | 290 | 95.4 | Steel-buckling |
| G2 | BF-H0.33-F1(5)-B1 | 245 | 7.9 | 307 | 18.1 | CFRP peeling |
| | BF-N0.50-F1(5)-B1 | 181 | 5.7 | 262 | 12.1 | CFRP peeling |
| | BF-H0.33-F1(5)-B2 | 253 | 8.2 | 375 | 51.0 | CFRP rupture |
| | BF-N0.50-F1(5)-B2 | 195 | 6.5 | 307 | 24.0 | CFRP rupture |
| G3 | BF-H0.33-F2(1)-B2 | 250 | 8.4 | 344 | 46.1 | CFRP peeling |
| | BF-H0.33-F2(1)-B2w | 260 | 8.6 | 347 | 48.7 | CFRP peeling |
| G4 | BF-H0.33-F1(1)-A1D1 | 240 | 7.3 | 323 | 43.9 | CFRP rupture |
| | BF-H0.33-F1(1)-A2D1 | 246 | 7.8 | 320 | 44 | Yield in ductile link followed by CFRP rupture |
| | BF-H0.33-F1(5)-A2D2 | 250 | 7.7 | 304 | 32 | CFRP premature rupture |

To summarize, it was concluded that the application of FRP for flexural strengthening of steel beams increases the yield moment. Using the new hybrid anchorage system reduced the FRP strains and increased the ultimate deflection capacity. In addition, the premature de-bonding of FRP material was delayed and prevented using the new system; hence, it was effective in this regard.

**Inverted-T Bent Cap Strengthened in Shear**

A structural safety concern in inverted-T bent caps is that, at service load unacceptable diagonal cracks frequently occur at the re-entrant corners between the cantilever ledges, flanges and the web. The service stress limits for different codes are summarized in the table below and these limits are set to avoid the development of inelastic deformation (ACI) and crack width limits not to be exceeded under service loads (TR55). Several research activities aimed at development of a serviceability design method that considers controlling and monitoring the cracks for newly constructed inverted-T bent caps; however, there is still a need to investigate possible methods to upgrade the possible non-ductile performance of existing ones.

Table 19: Service Stress Limits in Codes

| **CFRP** | **ACI (2008)** | **AASHTO (2012)** | **ISIS (2008)** | **TR55 (2000)** | **CNR (2004)** |
|---|---|---|---|---|---|
| | $0.55f_{fu}$ | $0.80f_{fu}$ | N/A | 0.65 | $0.80f_{fu}$ |

In addition, the behavior of an inverted T-beam is much more complicated than regular T-section beam. As mentioned before, the brittle failure in T-beams will occur due to shear failure, i.e. when the premature shear failure takes place without reaching the maximum flexural capacity of longitudinal rebars. In inverted-T girders, bearings on the top face of the flange of an inverted-T

girder produce vertical tensile forces (hanger tension) near the bottom of the web. Such forces are not ordinarily encountered in conventional T-beams, where vertical forces are applied at the top of the web. Furthermore, the longitudinal and lateral bending of the flange of an inverted-T girder produce a very complex stress distribution in the flange.

An experimental program to examine the effectiveness of new rehabilitation techniques using anchored carbon fiber reinforced polymer (CFRP) sheets to eliminate non-ductile failure mechanisms in hanger, web, and flange zones of RC inverted-T girders is reported here. Hanger failure involves the failure of the stirrups acting as hangers and supporting the concentrated loads on the bracket. Web failures involve web-shear or shear-compression failures and flange failures are attributed either to shear friction or flexure accompanied by punching shear in the bracket. A well-designed inverted-T girder should ensure that the load capacities of such non-ductile modes are higher than the load corresponding to the yielding of the longitudinal flexure reinforcement; otherwise, it should be retrofitted. Eight tests were conducted on four inverted-T ⅓rd scale girders under 4-point loading system. The control girders were subjected to increasing incremental load up to the first sign of non-ductile mechanism, while the rehabilitated specimens were tested up to failure. All the tested girders were identical in size and proportion, with the only difference being the reinforcement content in hanger, web shear and flange loading zones. The details regarding the span length, the dimensions and flexural reinforcement are shown in the figure below. It is noteworthy that, negligible capacities was provided in hanger, web-shear and punching zones (flanges) for girders G1&G2, G3 and G4, respectively in order to isolate the three different non-ductile mechanisms and to avoid the complications in the interpretations of the results in case of having two, or more, combined failure mechanisms.

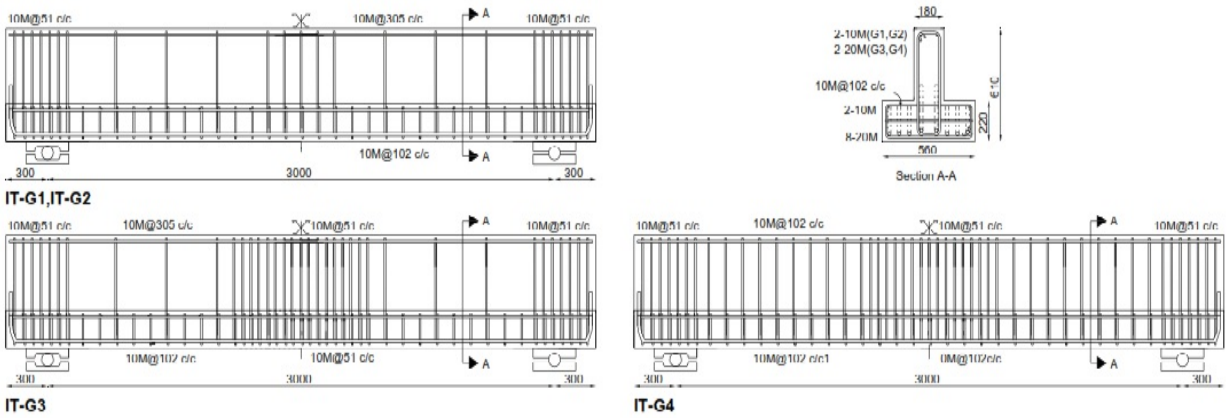


Figure 21: Dimensions and Details of Reinforcement of Control Girders (Galal and Sekar, 2007)

The control girders IT-G1 and IT-G2 were tested up to the first sign of non-ductile failure mechanism. The objective of control specimens IT-G1 and IT-G2 was to examine the effectiveness of two anchoring techniques, used in specimens IT-G1R and IT-G2R, to strengthen the hanger zone. Specimens IT-G3 and IT-G3R were tested to determine the feasibility of strengthening the web-shear zone of inverted-T girders using CFRP sheets. Specimens IT-G4 and IT-G4R aimed at investigating the feasibility of strengthening the punching zone in the flanges of inverted-T girders using CFRP sheets. The goal of all the proposed FRP-rehabilitation schemes is to increase the shear capacity of the governing non-ductile mechanism of the girder by adding the component, $V_{FRP}$, such that the rehabilitated girder would experience a ductile failure.

The girder IT-G1R was rehabilitated using 3 layers of CFRP sheets. At locations away from the loading plates (section A–A) holes with depth of 3″ were pre-drilled to allow for anchoring the FRP sheets. At the connection between the web and the flange, concave grout together with a thick curved angle plate were used to allow for the smooth transition of stresses in the FRP sheets and clamp the FRP in position. At locations of loading plates, it was not possible to extend the FRP sheets to the top of the flange; hence, two pre-drilled holes and CFRP fan-type anchors were used to transfer the stresses from the FRP to the girder.

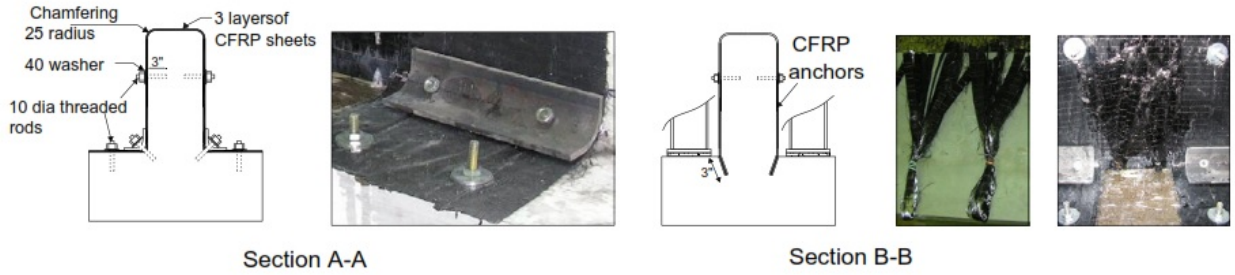


Figure 22: Rehabilitation Scheme for Girder IT-G1R (Galal and Sekar, 2007)

In specimen IT-G2R, another rehabilitation scheme was used in order to examine the effect of absence of anchors that are used in girder IT-G1R. The girder was rehabilitated using 3 layers of CFRP sheets that have an inverted-U shape over the web portion of the girder along the web shear zones and at the locations of the loading plates. Flange portion of the girder were also wrapped completely beneath and anchored on the top of the flange. The CFRP sheets were anchored using similar techniques used in IT-G1R except that fan-type anchors were not used in the loading zones. In order to eliminate the web-shear failure mechanism of girder IT-G3, the girder was rehabilitated using 3 layers of CFRP sheets with an inverted-U shape in the web shear zones. At the connection between the web and the flange, a curved angle plate was used similar to IT-G1R. Finally, to eliminate punching failure mechanism in the flange, 3 layers of C-shaped CFRP sheets were wrapped around the two flanges of the IT-G4R girder. In order to transfer the stresses from the CFRP wrap to the web of the girder, fiber anchors that were sandwiched between the layers of the CFRP wrap on both sides of the flange were embedded into the web. To increase the compression capacity of the web, 3 layers of CFRP sheet with an inverted-U shape were wrapped over the web up to half of the web height above the flange and were anchored with threaded rods.

The failure mode of the control specimens IT-G1 and IT-G2 tested in hanger zone was similar and was characterized by a non-ductile failure. On the other hand, the rehabilitated specimen IT-G1R had a higher load carrying capacity and behaved in a more ductile manner. Similarly the girder IT-G2R had a low stiffness but resulted in increase in the displacement ductility when compared to that of control specimen. Although it was expected that IT-G2R would have a ductile behavior that is similar (or even better) than that of IT-G1R (due to its higher FRP content), yet the absence of the fiber anchors at the loading zones resulted in a premature failure without achieving high ductility limits. This verifies the need for anchoring the FRP at the flange-web intersection zone. It can be said that, anchoring the CFRP sheets that are epoxied on the web or the flange into the girder using sandwiched (fan type) CFRP fiber anchors that are aligned with the CFRP sheets' fibers showed better performance compared to not using it in the loading zone.

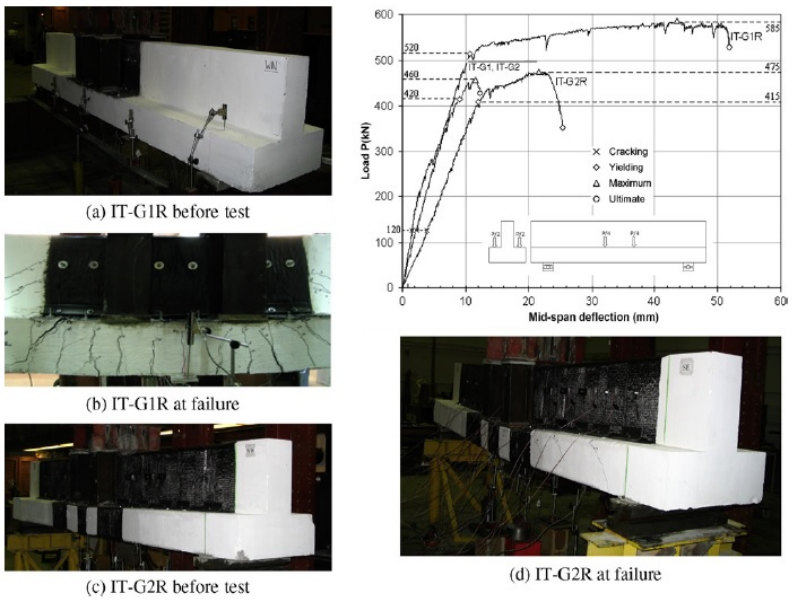


Figure 23: Failure and Load-deflection Relationship for Girders Rehabilitated in Hanger Zone (Galal and Sekar, 2007)

Girder IT-G3 did not show any increase in load carrying capacity. However, the rehabilitated girder (IT-G3R) failed at a higher load compared to the control specimen. The girder failed after reaching its flexural web-compression capacity. There were no signs of delamination of CFRP sheets from the concrete and they were fully bonded to the concrete at failure. The rehabilitation scheme was successful in eliminating the web-shear failure mechanism and increased the load carrying capacity of the girder. The reason that IT-G3R did not reach high displacement ductility level compared to IT-G1R, can be attributed to the lack of confinement of concrete in the web-compression zone (as this improvement was observed in girder IT-G4R).

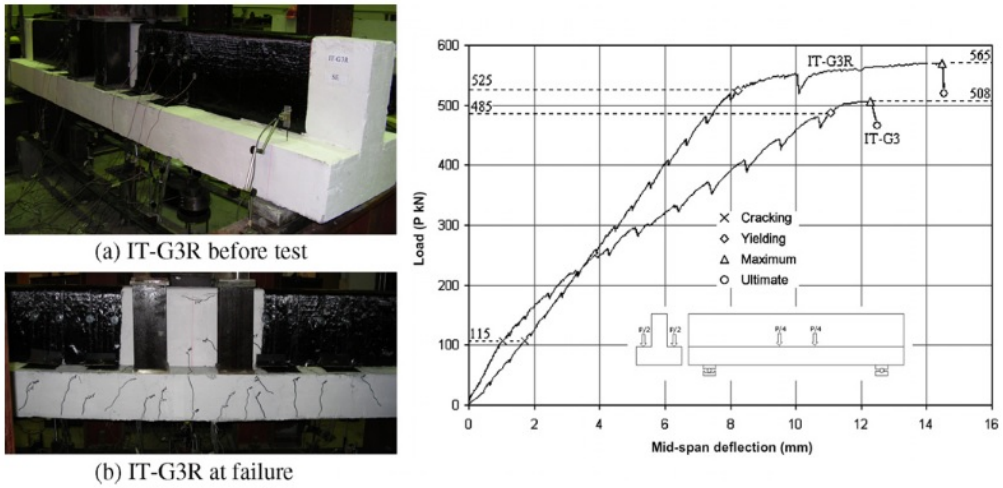


Figure 24: Failure and Load-deflection Relationship for Girder Rehabilitated in Web Zone (Galal and Sekar, 2007)

Girder IT-G4 failed due to non-ductile punching shear failure in the flange, while the rehabilitated girder ITG4R behaved in a more ductile manner with an increase in load bearing capacity and displacement ductility. This shows that the rehabilitation scheme was successful in eliminating the punching shear failure mechanism.

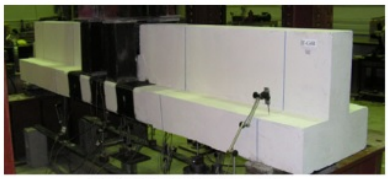

(a) IT-G4R before test

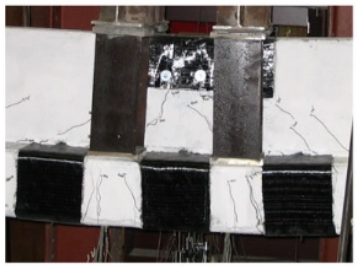

(b) IT-G4R at failure

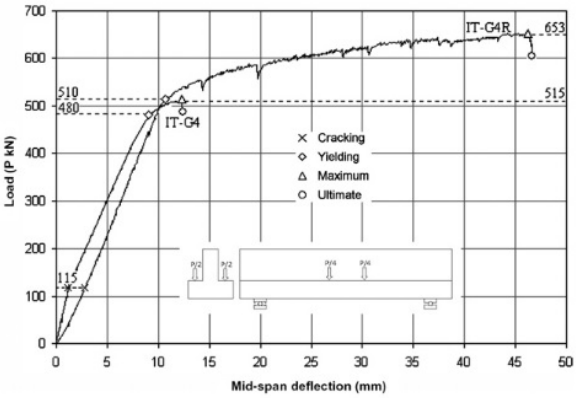


Figure 25: Failure and Load-deflection Relationship for Girder Rehabilitated in Flange Zone (Galal and Sekar, 2007)

The decrease in the stiffness, as well as the absence of initial stiffness up to the cracking point of concrete, for the rehabilitated girders (i.e. IT-G1R to IT-G4R) was expected due to the cracks formed upon loading the corresponding control specimens which resulted in a reduced stiffness of the rehabilitated ones upon reloading. Hence, it can be said that wrapping the girders with FRP did not contribute to their flexure stiffness, yet it increased the girders' capacities in the non-ductile modes, i.e. hanger, web, and flange, which consequently increased the girders' displacement ductility and load carrying capacities. Also, by calculating the $V_{nominal}$ using equations proposed by ACI and comparing with experimental shear capacity a very good agreement between experimental and analytical capacities was observed for all girders.

**Confinement Strengthening of Columns**

Short RC columns with low shear span/depth ratio, are vulnerable to brittle shear failure as repeatedly demonstrated during recent severe seismic events. It has been the practice to avoid the construction of short columns. However, many columns may have been originally designed as long columns but partial supporting walls were later constructed, changing them to short columns. Columns built prior to 1970 were designed on the basis of strength and according to the design procedures of the current codes might be considered as short columns. The objective of this experimental program is to evaluate the performance enhancement of short RC columns with high and low transverse reinforcement content when strengthened using glass or carbon composite materials and evaluate the viability of anchoring techniques to improve the confinement of square columns. Hence, the behavior of seven 2/3-scale square RC short columns strengthened using FRP was evaluated in 2 separate but dependent experimental programs. All the specimens had the same column overall dimensions and were divided in 2 groups. Group 1 was designed according to the

current Canadian Reinforced Concrete Design Code, while Group 2 was designed according to pre-1970 code. The longitudinal and shear reinforcement details are shown in the figure below.

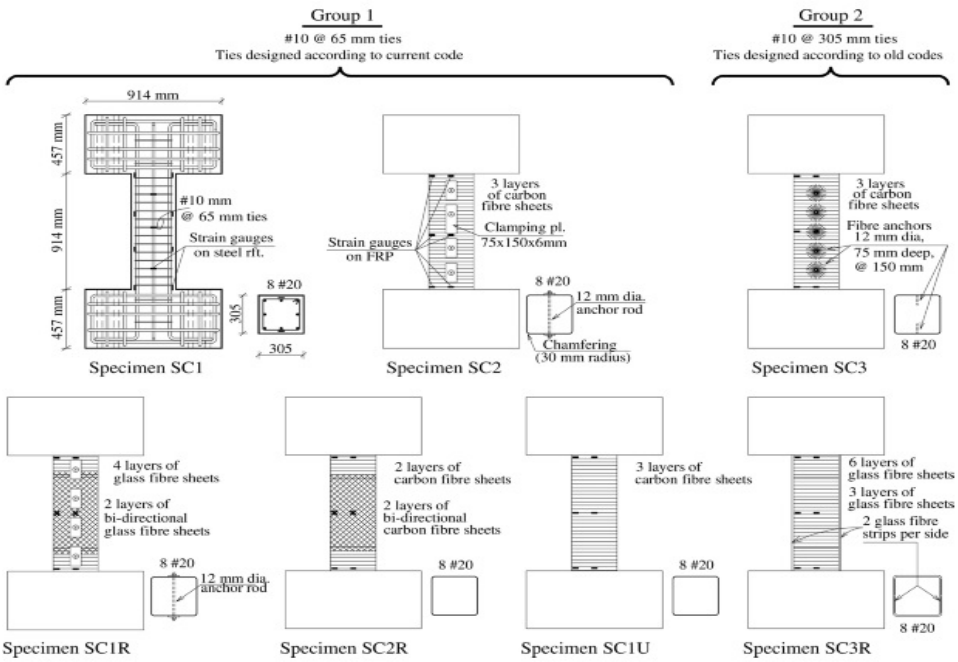


Figure 26: Dimensions, Details of Reinforcement and FRP Strengthening for the Specimens (Galal et al. 2005)

In Group 1, specimen SC1 was un-strengthened and was tested as the control specimen. The column SC2 was confined using three layers of CFRP. Four clamping plates and rods through the column section were used to reduce the potential bulging of the square sides of the column. SC1R strengthened using four layers of unidirectional glass fiber-reinforced polymer at the plastic hinge regions at the top and bottom ends of the column. Between the column end hinges two layers of bi-directional GFRP sheets were applied. Mechanical anchors similar to those used for specimen SC2 were used for SC1R. The amount of the GFRP at the plastic hinge location of SC1R was chosen such that it provides shear strength close to that provided by the CFRP of specimen SC2 to enable the evaluate the effect of FRP material on the response of RC short columns. Specimen SC2R was retrofitted using two layers of unidirectional CFRP at the plastic hinge zones and two layers of bi-directional CFRP in the intermediate zone. No anchors of the FRP sheets into the concrete were provided. The amount of CFRP at the plastic hinge location of SC2R was chosen to be less than that of specimen SC1U in order to evaluate the effect of number of FRP layers on the behavior of columns. Specimen SC1U was strengthened by three layers of CFRP, similar to specimen SC2 but without anchors so that the effect of anchoring can be evaluated. In Group 2, columns SC3 and SC3R had a low transverse reinforcement ratio selected to satisfy the minimum transverse reinforcement requirement according to 1968 ACI design practice. Column SC3 was strengthened using three layers of CFRP sheets. In this specimen five carbon fiber anchors were used in each of the two sides of the specimen. Column SC3R was retrofitted using six and three layers of unidirectional GFRP sheets at the plastic hinge zones and intermediate zone, respectively. The amount of the GFRP at the plastic hinge zone provides shear strength that is close to that provided by the three CFRP layers of specimen SC3. Two vertical GFRP strips were laid onto the loading and opposite sides of the column. The vertical GFRP strips were sandwiched between the

lateral GFRP confining sheets. The vertical strips were thought to provide an out-of-plane stiffness to the flexible sheets that are subjected to bulging of concrete and buckling of vertical reinforcement bars between transverse ties.

The columns were tested in the fixed–fixed end configuration and were subjected to cyclic displacements applied to the top end while the bottom end was fixed. The cyclic load represented lateral seismic forces while the vertical load represented gravity load on the column. The top and bottom ends of the column were fixed to the test set-up using a rigid reinforced concrete blocks. The test specimens were subjected to a 500 kN constant axial load. For all specimens, the lateral cyclic displacement level was selected as multiples of Δy with two cycles at each displacement level. The yield deflection was defined as the displacement at the top of the column when first yielding of the longitudinal bars occurs.

Figure 27: Test Set-up (Galal et al. 2005)

In group 1, column SC1 failed in shear. After the test, the GFRP wrapping was removed from the top and bottom parts of the column SC1R. The concrete under the fiber sheets at the plastic hinge location near the two ends of the column had several shear and flexure cracks. Yet the crack widths were small and the concrete remained functional due to the confining effect of the GFRP. The strengthening scheme used was successful in preventing the column shear failure, improving the ductility and strength of the specimen and developing flexural plastic hinges at the top and bottom of the column as compared with the control specimen SC1. In specimen SC2R, firstly the repeated loading cycles did not lead to significant loss of strength. However, at high displacement ductility levels, strength deterioration started due to the formation of new cracks and widening of the old cracks. Horizontal cracks in the concrete and separation between the fibers were observed together with the bulge of the fiber sheets in the compressed side of the column. At high levels of displacement ductility, pinching of the hysteretic loops due to development of shear cracks in the concrete and de-bonding of the FRP jacket was observed. The concrete under the FRP at the plastic hinge location at the two ends of the column was severely crushed. The strengthening scheme used was successful in preventing the column shear failure, improving the ductility and strength of the specimen and developing flexural plastic hinges at the top and bottom ends of the column as compared to the control specimen SC1. Specimen SC1U, unlike specimen SC2, showed signs of de-bonding between the CFRP wrap and the concrete column. This could be attributed to the absence of anchorage for the jacket. The ductile behavior of the specimen was due to the formation of plastic hinges at the column ends as a result of the increased shear capacity of the column.

In Group 2, column SC3R did not reach its full shear strength and exhibited limited ductility. This can be attributed to the bulging of the vertical GFRP strips on the compression side of the column, which reverses during cyclic loading. In fact, this bulging weakened the bond between the GFRP jacket and the column due to its imposed outward pressure on the jacket. In addition, the absence of mechanical anchorage between the GFRP jacket and the column expedited the de-bonding

between the jacket and the column. The column failed due to the formation of a wide diagonal shear crack at mid-height. This rehabilitation scheme failed to prevent the shear failure of the column because of the low modulus of elasticity of the unidirectional GFRP and the absence of an anchoring system for the fiber. The GFRP wrapping was removed from the column. The concrete under the fiber jacket had several diagonal shear cracks forming an X-pattern at the middle of the column and zigzag shapes near the edges

As long as the energy dissipation capacity is the matter of concern, all the strengthened specimens except for SC3R with low reinforcement, far out performed the control column SC1. The strains in the ties of the three strengthened specimens SC1R, SC2R, and SC3R at maximum drift were higher than the yield strain. On the other hand, the strain in the ties of the three rehabilitated specimens SC2, SC1U and SC3 did not reach the yield strain throughout the loading history. This indicates that the rehabilitation schemes used for specimens SC2, SC1U and SC3 were successful in providing adequate confinement and shear strength to allow the ductile hinging at the column ends to take place before shear failure. Furthermore, high FRP strains were recorded in columns SC2, SC1R, SC2R, SC1U and SC3 at the ultimate lateral displacement. This is a strong indication that the rehabilitation schemes used for these columns were successful in improving their performance, while the GFRP jacketing of column SC3R with low reinforcement ratio failed to achieve its objectives.

De-bonding occurred in the tested specimens SC2R, SC1U, and SC3R. Column SC2 showed a more ductile response without recognizable decrease in lateral force resistance, as compared to the response for column SC1U. In addition, comparing the dissipated energy capacity for the two specimens, indicates that the dissipated energy capacity of the anchored CFRP jacketed column is approximately 25% more than that of an identical column with an unanchored jacket. In SC2, anchoring the CFRP sheets to the concrete column decreased the strains in the transverse reinforcement and increased the strains in the CFRP as compared to the column SC1U, which was not provided with anchors. Anchoring FRP sheets to the concrete column may increase the cost of the rehabilitation scheme by approximately 20%. However, the associated performance enhancement would make the additional cost worthwhile.

Comparing the lateral force–displacement envelopes for specimens SC2 and SC3 indicated that at large lateral displacement, the column with the higher transverse steel content will have higher lateral load capacity due to improved confinement. Comparing the dissipated energy capacity for specimens SC2 and SC3 indicated that increasing the transverse steel content increases the dissipated energy capacity again due to the ductile behavior of the confined column. Comparing the tie strain and CFRP strain distribution along the height of columns SC2 and SC3 at ultimate lateral displacement indicated that increasing the transverse steel content decreases the tie strains at the column mid-height, while it has negligible effect on the tie strain at the column ends. On the other hand, increasing the transverse steel content reduced the strains in the FRP jacket along the column height. The ties at the top and bottom ends of the column are effective in confining the flexural hinge location while the ties near the mid-height of the column resist the shear. Comparing the lateral force–displacement envelopes for the specimens SC2R and SC1U indicated that increasing the number of FRP layers increased the column's shear capacity, which resulted in a more ductile response. The cumulative dissipated energy capacity for specimen SC1U with the larger number of FRP layers is higher than that of SC2R. Comparing the tie strain and CFRP strain distribution along the height of both specimens at ultimate lateral displacement indicated that

increasing the number of layers of CFRP sheets consistently decreases the strains in both the transverse steel ties and fiber sheets. The same benefits can be observed in Group 2 columns (pre-1970 columns).

Furthermore, column SC2 strengthened using CFRP had higher lateral force capacity and energy dissipating capacity as compared to column SC1R that was strengthened using GFRP. Comparing the tie strain and CFRP strain distribution along the height of both test columns at ultimate lateral displacement indicated that in the case of CFRP jackets the strains in the steel ties and the FRP along the column height decreased. This is due to the high modulus of elasticity of the carbon fiber material as compared to the glass fiber material. The poor confinement of the glass fiber jacket allowed the cracks in the concrete to widen with the consequence of de-bonding of the fiber and loss of shear resistance. The difference in behavior between the two materials is consistent along the height of the column.

From the test results, the most appropriate strengthening technique for short columns was found to be the use of anchored CFRP jackets over the height of the column and the additional confinement of the end flexural hinge zones using CFRP sheets with unidirectional hoop fiber orientation.

**Shear Wall Upgrade Using FRP Strengthening**

Shear walls that were designed according to older codes may now be seismically deficient according to modern design codes. Also, shear walls designed according to modern codes may experience higher demands at upper stories arising from the effects of higher modes of vibrations and these demands were not accounted for in their initial design. Hence, upgrades may be needed at conventional plastic hinge zones at the base of a wall or at higher stories as a result of the unaccounted effects of higher modes of vibration with aim to improve the strength, stiffness, and ductility, or a combination of these characteristics.

In a research previously conducted at the EPM (Ecole Polytechnique de Montréal) by Ghorbanirenani et al. (2012), two 8-story reduced size shear walls were tested where the ground motion was simulated by shake table. The aim was to experimentally investigate the effect of higher modes of vibration on multistory RC shear walls subjected to eastern North American ground motions, which are expected to be rich in high frequencies. Tests on the original walls showed the formation of a plastic hinge at the sixth-story level, in addition to the one at the wall base. In a separate but dependent research by El-Sokkary et al. (2013), the original walls were rehabilitated by using CFRP sheets at the two locations that experienced nonlinear response. The aim of the rehabilitation scheme for the two walls was to increase the flexural and shear capacities of the wall at the sixth story panel as a result of the observed increase in demand at that level, whereas the base panel was confined by using CFRP sheets to increase the ductility without increasing the flexural strength. The rehabilitated walls were subjected to the same ground motion record applied at the base of the original walls. Although the ground motion records used in the shake table tests reached 200% of the design ground motion, the capacity of the original walls and the FRP retrofitted walls was not reached. Therefore, there was a need to conduct cyclic tests on RC shear wall panels that represent the sixth story panel of the eight-story RC walls to evaluate its full performance up to failure and assess the efficiency of the FRP retrofit schemes.

The objective of the current study is to investigate experimentally the effectiveness of using externally bonded CFRP composite sheets to increase the flexural and shear capacities of RC shear walls that are susceptible to increased demands. The walls represent the sixth story panel of an eight-story RC, moderately ductile, shear wall designed according to the 2005 National Building Code of Canada (NBCC 2005). Three RC shear walls were tested under cyclic loading up to failure. The tested walls represent a control wall and two walls retrofitted with FRP by using two different retrofit schemes. The three walls were tested under constant axial load and with increasing cycles of synchronized top moment and lateral load. The aim was to evaluate the complete performance of the rehabilitated walls up to failure.

The plastic hinge region of a wall or the location that requires retrofitting could be tested by taking into account the effect of the shear wall panels above and below the test panel. The remaining stories were assumed to behave in an elastic manner. A rigid reinforced concrete top block was poured monolithically with the wall and the bottom footing. The top rigid block ensured the uniform transfer of axial load, bending moment, and shear force to the wall section. The bottom rigid block was anchored to the strong floor of the lab. Three hydraulic actuators mounted against a steel reaction frame were used. Two actuators were placed vertically to allow the application of axial load and in-plane moment at the top of the wall. A horizontal actuator was used to apply the shear force at the top of the wall. A rigid steel I-beam was used to uniformly transfer the actuator forces to the top of the wall. The vertical actuators were controlled in force control mode based on the feedback from the load cell in the horizontal actuator while the horizontal actuator was controlled in the force mode up to wall yielding, after this the control was switched to displacement mode. The shake table tests conducted on the eight-story walls found that the factored moment at the sixth story, $M_f$, was almost 17% greater than the design factored resistance, $M_r$, when subjected to the design ground motion. Therefore, the retrofit design strategy required that the factored resistance of the retrofitted walls to be at least 1.17 times that of the control wall. A value of 1.25 was selected in the design of RW1 and RW2.

The retrofit scheme of RW1 aimed at increasing the flexural capacity of the wall section by applying vertical CFRP sheets at the boundary zones of the wall. This was achieved by applying a 200mm-wide vertical unidirectional CFRP strip at the wall extremities on both faces. The expected failure mode of the retrofitted wall used in the estimation of the ultimate load was failure of the CFRP vertical sheet system after reaching the design strain. The vertical FRP strips were anchored to the top and bottom blocks by using FRP fan anchors. Two anchors were used for each strip on each wall face at the top and at the bottom. First, the CFRP anchors were securely inserted into the end blocks and the fans were spread on the concrete wall, and then the vertical CFRP strips were applied. Horizontal CFRP sheets were applied on top of the vertical CFRP strips to increase the shear capacity of the wall. Also, two C-shaped CFRP sheets overlapped at the boundary regions of the wall to provide a confinement of the wall end columns.

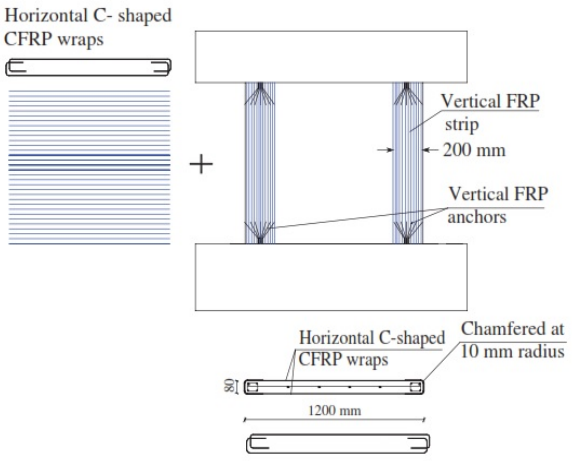


Figure 28: FRP-retrofitted Wall RW1 (El-Sokkary and Galal, 2013)

In the second retrofit scheme, instead of using vertical and horizontal CFRP sheets to enhance the flexural and shear behavior of the wall, respectively, diagonal CFRP strips were applied on each face of the wall panel. This results in an inclined force that can be resolved into vertical and horizontal components. The vertical component of the force is transferred to the top and bottom blocks by using FRP anchors. The horizontal component was resisted by applying two 200mm-wide horizontal C-shaped wraps near the top and bottom blocks of the wall. The width of the diagonal strip was selected to be 280mm so that the effective cross-sectional area of the inclined fibers be close to that of the 200mm-wide vertical strip used in the first retrofit scheme. An advantage to this layout of CFRP sheets is that it makes the wall cracks visible; hence, the retrofitted wall can be monitored after retrofit. Also, this scheme used less FRP composite material than that of RW1.

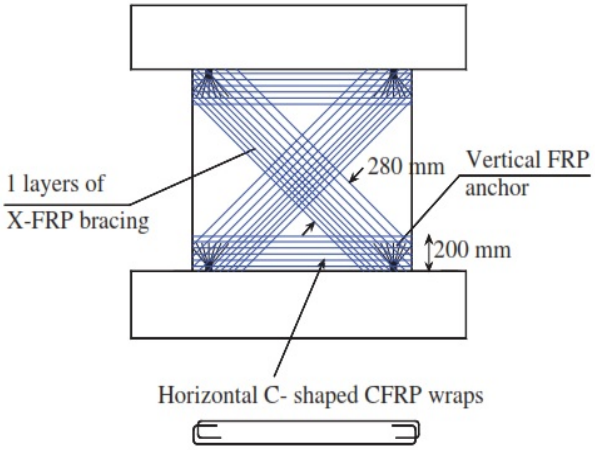


Figure 29: FRP-retrofitted Wall RW2
(El-Sokkary and Galal, 2013)

The CW panel was tested by applying lateral load push and pull cycles at the top of the wall in a force-control mode. After reaching the yielding load, the control mode was switched from force control to displacement control, and the wall was subjected to increasing cyclic displacements. The wall displacement at yield was measured during the test based on the lateral displacement of the wall at the yield strain of the extreme flexural bar. After the yielding load, the wall showed a gain in its strength upon increasing the lateral displacement due to the strain hardening of the flexural steel reinforcement. When the wall yielded, more horizontal fine cracks were observed and began to propagate. These cracks did not widen, whereas it was observed that only the base crack became wider with the increased displacement of the wall. Concrete crushing was observed at the toe of the wall on the compression side. Minor buckling of vertical bars occurred at the final stage as a result of the exposure of bars after concrete crushing of the wall toes. The failure mechanism of the control wall was the rupture of the extreme flexure reinforcement bars, accompanied by concrete crushing of the wall toes.


Figure 30: Crack Pattern at Failure, Concrete Toe Crushing and Lateral load-top Displacement of CW (El-Sokkary and Galal, 2013)

RW1 was tested by applying lateral loads at the top of the wall in force control mode to check the proper functioning of the instrumentation. The load was increased in force control mode until the load that corresponded to the yielding of flexure reinforcement was reached. After reaching the yield point, the wall was tested in displacement control mode up to failure. The wall was subjected to cyclic displacements with increasing displacement ductility levels. After reaching the yield load, the wall started to gain strength with a relatively high stiffness (compared to CW) upon increasing the cyclic lateral displacement. This type of gain is attributable to the contribution of the vertically anchored FRP strips. The FRP strips were stretched when the wall was pushed in one direction, and were compressed when the load was reversed. At the maximum lateral load level, cracking of the wall footing near the FRP anchors started to propagate, which marked the beginning of a local footing failure as a result of pullout of the FRP anchors. The bar rupture was delayed as a result of the flexural strength added by the vertical FRP sheets and the presence of FRP anchors in the initial stages. Therefore, there was no steel reinforcement failure before the FRP anchors were fully pulled out. The test was stopped when severe damage of the wall footing happened and before reaching the rupture of extreme vertical steel bars. No rupture of FRP anchors or FRP sheets was observed. The full wrapping of RW1 along its height resulted in relocating the plastic hinge toward the support. The failure mode of RW1 was pullout of the FRP anchors at the wall base, accompanied by a local concrete cone failure of the wall footing.

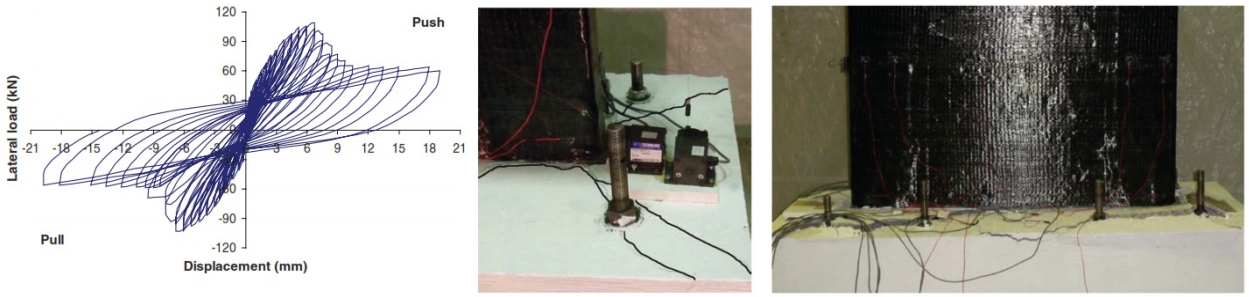


Figure 31: Lateral Load-top Displacement, Local Cracking of Footing at the Maximum Load and Failure of RW1 (El-Sokkary and Galal, 2013)

The loads applied on RW2 exactly similar to RW1. After reaching the yield load, the wall continued to gain strength with relatively high stiffness as a result of the contribution of the diagonal FRP strips and the strain hardening of the flexural steel reinforcement. Upon cyclic loading, several cracks developed in the wall. Upon increasing the cyclic displacement of the wall, no further crack propagation occurred, but the existing cracks widened. It is believed that widening of the primary crack above the horizontal CFRP strip and its opening and closure during successive cycles resulted in maintaining a relatively stable lateral load resistance of the wall while increasing its ductility and energy dissipation capacity. Crushing of the concrete above the well-confined end zones by means of the horizontal CFRP wraps was noticed, and a small portion of the diagonal FRP strip started to rupture. The failure mechanism of RW2 was identified as a rupture of the diagonal FRP strips resisting the pull cycles and pullout of the FRP anchors resisting the push cycles. The failure was characterized by concrete crushing above the confined concrete zone wrapped with horizontal CFRP wraps and buckling of the vertical steel reinforcement bars at both sides of the wall. Because the wall was not fully wrapped along its full height, the plastic hinge was able to form above the horizontal FRP wraps near the wall base. This led to crushing of concrete at the wall boundaries, which resulted in a lack of restraint of buckling to the vertical steel reinforcement

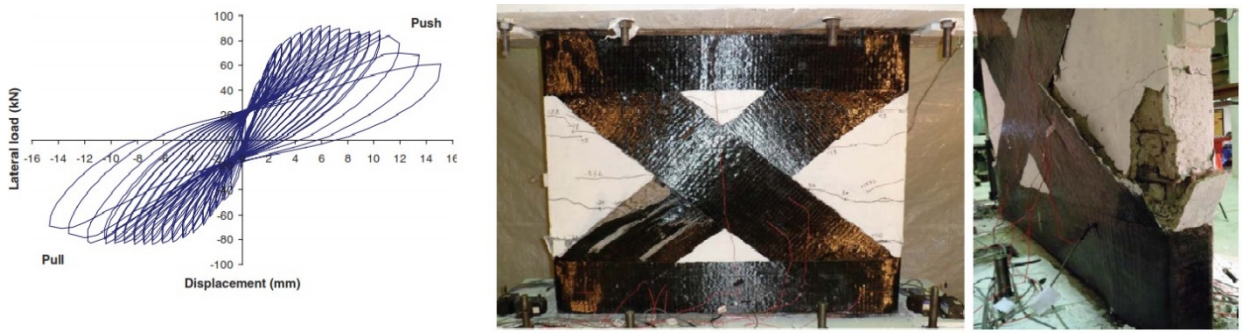


Figure 32: Lateral Load-top Displacement, Rupture of Diagonal FRP and Concrete Crushing and Buckling of Flexure Reinforcement of RW2 (El-Sokkary and Galal, 2013)

The envelope of the lateral load-drift ratio relationships for the three tested walls shows that the control wall was characterized by ductile behavior. RW1 showed an increase of 80% in the flexural capacity compared to CW, accompanied by a decrease in the displacement ductility of the wall. The yield load was measured at 46% higher than CW at a 7% higher yield displacement. The primary target of the retrofit scheme for RW1 was to increase the flexural capacity of the wall at levels that were subjected to demands higher than those in the design. Therefore, the ductility of the wall is considered to be a secondary parameter that can be overlooked. RW2 showed a 50% increase of flexural capacity compared to CW, accompanied by similar displacement ductility. The yield load was 19% higher than that of CW at 7% higher yield displacement. RW2 was designed to have the same flexural capacity of RW1. Interestingly, RW2 was found to have less flexural capacity with much higher displacement ductility. This favorable behavior of RW2 combines the two primary advantages of the other wall panels: the high strength of RW1 and the high ductility of CW without sacrificing the energy dissipation capacity. The flexural capacity of RW2 was measured to be less than the capacity of RW1 because both diagonal FRP strips for RW2 were stretched while the wall was pushed (or pulled). This is different than the behavior of RW1, in which the vertical FRP strips were stretched on one side of the wall while compressed on the other side. This specific behavior of RW2 is attributed to the wide cracks propagated between the top and bottom horizontal CFRP wraps along the height of the wall. These wide cracks did not close completely when the load reversed and the concrete came under compression, which resulted in a residual elongation of the FRP diagonal strips. In fact, the FRP strips were acting against each other. The accumulation of permanent strains in the flexure steel reinforcement, the opening of horizontal cracks in RW2 above the horizontal FRP strips, and the ability of the diagonal FRP strips to stretch as the cracks widen allowed RW2 to sustain high lateral displacements while maintaining its strength. On the other hand, the vertical CFRP strips of RW1 controlled the opening of horizontal cracks of RW1 because the cracks were normal in the fiber direction, resulting in a lower displacement ductility capacity of the wall.

The experimental nominal capacities of RW1 and RW2 were higher than those calculated by using section analysis and strain compatibility at the same net strains measured during the tests. The difference between the experimental and predicted capacities implies that the tensile force resisted by the FRP strips was almost 160% higher than that predicted based on the manufacturer data sheet. This indicates that the retrofit scheme used for RW2 was able to improve the overall rotational ductility capacity of the wall while increasing its flexural capacity. Therefore, such a retrofit scheme will be efficient in the retrofit of multistory RC walls at the plastic hinge regions.

**Limitations, Future Challenges and Additional Considerations**

As discussed before, there exist variety of codes for FRP strengthening of structural members. Factors such as levels of accuracy, ease of use and format compatibility should be considered when the selection of a design code / guide is the matter of concern. Comparison of various codes shows that there are differences in the outcomes, and this is mainly due to making different assumptions in defining reduction factors. Hence, more research is required to unify the codes and develop an internationally accepted design standard that allows rational design in a reliable manner.

Furthermore, it could be claimed that the initial cost of FRP material is not competitive with traditional material used for bridge strengthening. Although field applications has proven that from a long-term economic standpoint this dis-benefit is outweighed by numerous benefits, the owners and authorities usually tend to select the material based on short-term economy and safety benefits regardless of the fact that material cost in a bridge rehabilitation project rarely exceeds 20% of the total cost. Consequently, one should acknowledge that the comparison of the various competing alternatives should be based on establishing and estimating the whole life costs, from onset to decommissioning and this can be done only under the umbrella of life cycle cost analysis. That being said, the initial cost of the structure can be found in a straightforward manner but the prediction of rehabilitation and maintenance costs and intervals is very difficult and requires a lot of expertise and engineering judgment with enough knowledge of bridge management systems and concepts such as reliability and risk-based decision analysis.

The effect of environmental conditions on FRP used for strengthening of bridge elements remains a major concern as well. Sub-zero temperatures can change the mechanical properties of FRP material while high temperatures and humidity can severely deteriorate the FRP. Progressive damage of the bridges is attributable to presence of the deicing salts, cycles of freeze-thaw, high alkalinity, wet-dry cycles and extreme temperatures in the summer and winter. Codes often use reduction factors to account for degradation over time due to environmental effects. Additionally, when the effect of environmental conditions are coupled with loading conditions the caution should be doubled.

Constant loads over a time can decrease the endurance time (increase the ratio of sustained tensile stress to the short-term strength of the FRP) and this will lead to creep rupture. The phenomenon of creep in operating bridges is so serious that it is sometimes the case that the creep-rupture stress limits actually govern the FRP strengthening design. The stress levels in the FRP laminate should be checked to avoid the failure of the FRP due to cyclic stresses and fatigue as well. Codes often limit the difference between maximum and minimum stresses to guard against fatigue, and this varies significantly in various codes. Special design considerations such as impact and fire resistance may also be relevant.

In summary, the introduction of FRP as an innovative material for bridge strengthening offers huge advantages over the traditional retrofit schemes. However, all the conclusions drawn are based on a limited number of tests and more tests and analyses should be conducted to generalize the aforementioned conclusions. The increase in experience with various FRP strengthening schemes and the wide-spread adoption of the material in the bridge retrofit industry requires more research to unify the design codes, justify the use of FRP from economical point of view and address fundamental issues such as durability, creep and fatigue.

**Acknowledgements**

First and foremost, I would like to thank my research students. None of this research work would have materialized without them. A special thanks to Mr. Pedram Pakzad for assisting with assembling this paper. Finally, I would like to thank the funding agencies (Natural Sciences and Engineering Research Council of Canada, NSERC; le fonds de recherche du Québec – nature et technologies, FRQNT; and Canada Foundation for Innovation, CFI) and the industrial partners (Fyfe Co.) for their financial and in-kind support for conducting the experimental and numerical studies.

**Notations**

**AASHTO (2012)**

$f_c'$ = 28 - day compression strength of the concrete (ksi)
$R_r$ = factored resistance
$\eta_i$ = load modifier
*DC* = load effect due to component and attachments
*DW* = load effect due to wearing surfaces and utilities
*LL* = live load effect
*IM* = force effect due to dynamic load allowance
$f_{peel}$ = peel stress at the FRP reinforcement concrete interface (ksi)
$\varepsilon_{frp}^{u}$ = strain developed in the FRP reinforcement at the ultimate limit state
$\varepsilon_{frp}^{y}$ = strain in the FRP reinforcement at the point where the steel tension reinforcement yields
$M_r$ = factored resistance of a steel-reinforced concrete rectangular section strengthened with FRP reinforcement externally bonded to the beam tension surface (kip-in)
$A_s$ = area of non-prestressed tension reinforcement ($in^2$)
$f_s$ = stress in the steel tension reinforcement at development of nominal flexural resistance (ksi)
$Z$ = lever arm length
$d_s$ = distance from extreme compression surface to the centroid of non-prestressed tension reinforcement
$k_2$ = multiplier for locating resultant of the compression force in the concrete
c = depth of the concrete compression zone (in)
$A_s'$ = area of compression reinforcement ($in^2$)
$f_s'$ = stress in the steel compression reinforcement at development of nominal flexural resistance (ksi)
$T_{frp}$ = tension force in the FRP reinforcement
$\phi_{frp}$ = resistance factor for FRP component of resistance
$h$ = depth of section; overall thickness or depth of a member
$V_u$ = factored shear force at the reinforcement end-termination (kips)

$S_{max}$ = maximum spacing of FRP reinforcement
$d_v$ = effective shear depth
$b_v$ = effective shear web width (in)
$V_p$ = component of the effective prestressing force in the direction of applied shear (kips)
$V_{frp}$ = the nominal shear strength provided by the externally bonded FRP reinforcement (kips)
$\rho_f$ = FRP reinforcement ratio
$E_f$ = modulus of the FRP reinforcement in the direction of structural action
$\varepsilon_{fe}$ = effective strain level in FRP reinforcement attained at failure, in/in (mm/mm)
$d_f$ = effective FRP shear reinforcement depth
$\alpha_f$ = angle of inclination of FRP with respect to the longitudinal axis of the member
$V_n$ = nominal shear strength
$\varepsilon_{fu}$ = ultimate rupture strain of FRP reinforcement
$R_f$ = Reduction factor
$f_l$ = ultimate confinement pressure due to FRP strengthening (ksi)
$N_{frp}$ = number of plies of FRP reinforcement
$D$ = diameter of compression member of circular cross section, in (mm)
$k_e$ = strength reduction factor applied for unexpected eccentricities
$P_r$ = factored axial load resistance (kips)
$f'_{cc}$ = compressive strength of confined concrete (ksi)
$A_g$ = gross area of column section ($in^2$)
$A_{st}$ = total area of longitudinal steel reinforcement ($in^2$)
$f_y$ = specified yield stress of steel reinforcement (ksi)
$\varepsilon_{fd}$ = de-bonding strain of externally bonded FRP reinforcement, in/in (mm/mm)
$\varepsilon_t$ = net tensile strain in extreme tension steel at nominal strength, in/in (mm/mm)
$\varepsilon_{sy}$ = strain corresponding to yield strength of non-prestressed steel reinforcement, in/in (mm/mm)
$\varepsilon_c$ = strain in the concrete
η = creep rupture reduction factor
$T_{frp}$ = tensile force in the FRP reinforcement corresponding to an FRP strain of 0.005
$\tau_{int}$ = interface shear transfer
$b_{frp}$ = width of the FRP reinforcement (in.)
$L_d$ = development length

**ISIS (2008)**

$S_{DL}$ = service dead load
$S_{LL}$ = service live load
$\phi$ = resistance factor
$R_n$ = structural design capacity

$\varepsilon_{frp}$ = strain in FRP reinforcement

$S_{frp}$= spacing of externally-bonded FRP bands on concrete for shear strengthening measured along the axis of the member or unit width (i.e., 1.0) of a continuous FRP shear reinforcement, mm

$W_{frp}$ = width of FRP sheet measured perpendicular to the direction of main fibers, mm

$d_{frp}$ = effective shear depth for FRP, calculated similar to dv for steel reinforcement in accordance with Clause 8.9.1.5 of CSA S6-06, or the distance from extreme compression fibre to centroid of tension FRP reinforcement, mm

$V_c$ = factored shear resistance attributed to the concrete, N

$V_s$= factored shear resistance provided by steel shear reinforcement, N

$V_{FRP}$ = factored shear resistance provided by FRP shear reinforcement, N

$b_v$ = effective web width within depth dv, mm

$d_v$= S6-06: the effective shear depth for internal steel, as defined in Clause 8.9.1.5 of CSA S6-06, mm

$f_c'$ = specified compressive strength of concrete, MPa

$E_{frp}$ = modulus of elasticity of FRP, MPa

$\phi_{frp}$ = resistance factor for FRP

$A_{frp}$ = area of cross-section of an FRP bar, plate, sheet or tendon, $mm^2$

$d_{frp}$ = effective shear depth for FRP, calculated similar to dv for steel reinforcement in accordance with Clause 8.9.1.5 of CSA S6-06, or the distance from extreme compression fibre to centroid of tension FRP reinforcement, mm

$\beta$ = angle of inclination of the transverse reinforcement to the longitudinal axis of the member

θ = angle of inclination of the principal diagonal compressive stress to the longitudinal axis of the member

$V_r$ = factored shear resistance, N

$\varepsilon_{FRPe}$ = effective strain in FRP reinforcement

$\varepsilon_{FRPu}$ = ultimate strain in FRP reinforcement

$P_r$ = factored axial load resistance, N / factored axial resistance of a section in compression with minimum eccentricity, N

$\alpha_1$ = ratio of average stress in rectangular compression block to the specified concrete compressive strength

$f_{IFRP}$ = confinement pressure due to FRP strengthening at the ULS, MPa

$t_{frp}$ = total thickness of externally-bonded FRP plates or sheets, mm

$l_a$ = minimum required anchorage length for externally-bonded FRP beyond the point where no strengthening is required, mm

$f_{FRPu}$ = specified tensile strength of an FRP bars, plates, sheets, or tendons, MPa

**ACI (2008)**

$R_n$ = nominal strength of a member
$S_{DL}$ = service dead load
$S_{LL}$ = service live load
$V_u$ = factored shear
$V_c$ = nominal shear strength provided by concrete with steel flexural reinforcement, lb (N)
$\varepsilon_{fd}$ = de-bonding strain of externally bonded FRP reinforcement, in/in (mm/mm)
$E_f$ = tensile modulus of elasticity of FRP, psi (MPa)
$n_f$ = number of plies of continuous fiber sheets
$t_f$ = nominal thickness of one ply of FRP reinforcement, in (mm)
$\varepsilon_{fu}$ = ultimate FRP strain
$M_n$ = nominal flexural strength, in-lb (N-mm)
$A_s$ and $A_f$ = areas of tension material (steel and FRP)
$f_s$ = stress in non-prestressed steel reinforcement, psi (MPa)
$f_{fe}$ = effective stress in the FRP; stress level attained at section failure, psi (MPa)
$d - \beta_1 c/2$ and $h - \beta_1 c/2$ = lever arms to the compression zone of the concrete
$d$ = distance from extreme compression fiber to centroid of tension reinforcement, in (mm)
$\beta_1$ = ratio of depth of equivalent rectangular stress block to depth of the neutral axis
c = distance from extreme compression fiber to the neutral axis, in (mm)
$h$ = overall thickness or height of a member, in (mm)
ψ = reduction factor for FRP sheet
$\varepsilon_t$ = net tensile strain in extreme tension steel at nominal strength, in/in (mm/mm)
$\varepsilon_{sy}$ = strain corresponding to yield strength of non-prestressed steel reinforcement
$d_{frp}$ = effective FRP shear reinforcement depth
$W_{frp}$ = width of FRP reinforcing plies, in (mm)
$S_{frp}$ = spacing of FRP reinforcement
$V_s$ = nominal shear strength provided by steel stirrups, lb (N)
$V_f$ = nominal shear strength provided by FRP stirrups, lb (N)
$b_w$ = web width or diameter of circular section, in (mm)
$S_{max}$ = maximum spacing of FRP reinforcement
$A_f$ = area of FRP external reinforcement, $in^2$ ($mm^2$)
$d_f$ = effective depth of FRP flexural reinforcement, in (mm)
$d_{fv}$ = effective depth of FRP shear reinforcement, in (mm)
$S_f$ = Spacing between adjacent FRP strips
$V_n$ = nominal shear strength, lb (N)
$\varepsilon_{fe}$ = effective strain level in FRP reinforcement attained at failure, in/in (mm/mm)
$K_v$ = bond-reduction coefficient (bond-dependent coefficient for shear)

$\varepsilon_{ccu}$ = ultimate axial compressive strain of confined concrete corresponding to 0.85*fcc*′ in a lightly confined member (member confined to restore its concrete design compressive strength), or ultimate axial compressive strain of confined concrete corresponding to failure in a heavily confined member
$\varepsilon_c'$ = maximum strain of unconfined concrete corresponding to, in/in (mm/mm); may be taken as 0.002
$K_b$ = factor accounting for the geometry of the section (1.0 for circular cross sections) / efficiency factor for FRP reinforcement in determination of $\varepsilon_{ccu}$
$f_l$ = maximum confining pressure due to FRP jacket, psi (MPa)
$f_{cc,u}'$ = ultimate compressive strength of confined concrete, psi (MPa)
$E_2$ = slope of linear portion of stress-strain model for FRP-confined concrete, psi (MPa)
$P_n$ = nominal axial compressive strength of a concrete section, lb (N)
$f_{cc}'$ = compressive strength of confined concrete, psi (MPa)
$K_a$ = efficiency factor for FRP reinforcement in determination of $f'_{cc}$ (based on geometry of cross section)
$f_{f,s}$ = fiber stress limits under service conditions
$f_{fu}$ = ultimate stress of FRP
$l_{df}$ = critical length over which the bond capacity of FRP is developed

**JSCE (2001)**

$\sigma_f$ = peeling stress
$G_f$ = fracture energy factor
$E_f$ = modulus of elasticity for continuous fiber sheet (N/mm2)
$n_f$ = number of plies of continuous fiber sheets
$t_f$ = thickness of one layer of continuous fiber sheet (mm)
$V_{fd}$ = effective FRP design shear strength
$K$ = shear reinforcing efficiency of continuous fiber sheets
$f_{fud}$ = design tension yield strength of FRP
$A_f$ = total cross-sectional area of FRP
$\alpha_f$ = angle formed by FRP about the member axis
$S_f$ = spacing of FRP
Z = lever arm length
$\gamma_b$ = member factor (generally may be set to 1.15)
$V_{fyd}$ = Total shear capacity
$V_{cd}$ = shear resistance of concrete
$V_{sd}$ = shear resistance of steel

$\mu$ = Reduction factor resulting from the influence of fatigue load on the interfacial fracture energy relating to the bond of continuous fiber sheets to concrete

**CNR (2004)**

$\tau_{be}$ = equivalent shear stress at the adhesive-concrete interface

$f_{b,d}$ = design bond strength between FRP reinforcement and concrete (or masonry)

$\varepsilon_{fd}$ = maximum FRP tensile strain (design strain of FRP reinforcement)

$\varepsilon_{fk}$ = characteristic value of the adopted strengthening system (characteristic rupture strain of FRP reinforcement)

$\eta_a$ = environmental factor

$\gamma_f$ = partial factor for FRP rupture

$\varepsilon_{fdd}$ = maximum strain due to intermediate de-bonding (maximum strain of FRP reinforcement before debonding)

$W_f$ = width of FRP laminate

$\rho_f$ = spacing of FRP strips or discontinuous FRP U-wraps

$V_{Rd,max}$= maximum concrete contribution to the shear capacity

$f_{cd}$ = design concrete compressive strength

$d$ = distance from extreme compression fiber to centroid of tension reinforcement

$V_{Rd,f}$= FRP contribution to the shear capacity

$\gamma_{Rd}$ = partial factor for resistance models

$h_w$ = stem depth

$f_{fed}$ = effective FRP design strength

$t_f$= thickness of the adopted FRP system

$\beta$ = angle of inclination of the transverse reinforcement to the longitudinal axis of the member

$\theta$ = angle of inclination of the principal diagonal compressive stress to the longitudinal axis of the member

$V_{Rd}$= shear capacity of FRP-strengthened member

$V_{Rd,ct}$= concrete contribution to the shear capacity

$V_{Rd,s}$= steel contribution to the shear capacity

$\varepsilon_{fd,rid}$ = reduced design strain of FRP reinforcement for confined members

$f_{l,eff}$= effective confining pressure

$f_{ccd}$ = design strength of confined concrete

$\varepsilon_{ccu}$ = design ultimate strain of confined concrete

$N_{Rcc,d}$= axial capacity of FRP-confined concrete member

$A_c$ = area of concrete cross-section, net of steel reinforcement

$f_{fyd}$ = design yield strength of longitudinal steel reinforcement

$f_{cd}$ = design concrete compressive strength

$\eta_1$ = conversion factor for long term effects
$l_e$ = optimal bond length
$f_{ctm}$ = mean value of concrete tensile strength

**TR55 (2000)**

$M_r$ = design resistance moment of strengthened section
$F_s$ = tensile force in steel reinforcement
z = lever arm
$F_f$ = tensile force in FRP
h = overall depth of member
d = effective depth of section
$\gamma_{mm}$ = partial safety factor for manufacture of FRP
$\gamma_{mf}$ = partial safety factor for strength of FRP
$\gamma_{mF}$ = partial safety factor for FRP
$f_{cu}$ = characteristic compressive cube strength of concrete
$V_{Rf}$ = shear resistance of FRP
$A_{fs}$ = area of FRP shear reinforcement
$E_{fd}$ = design elastic modulus of FRP
$\varepsilon_{fe}$ = effective FRP strain
$\beta$ = angle between FRP and the longitudinal axis of the member
$d_f$ = effective depth of FRP shear reinforcement
$S_f$ = spacing of FRP strips (for continuous sheet reinforcement $S_f = W_{fe}$)
$W_{fe}$ = effective width of FRP
$f_{ccd}$ = design confined concrete compressive strength
$\gamma_{mc}$ = partial safety factor for concrete
$t_f$ = thickness of FRP
$D$ = diameter of column
$l_{t,max}$ = maximum anchorage length
$f_{ctm}$ = tensile strength of concrete

**References**


1. AASHTO (2012). “Guide Specifications for Design of Bonded FRP Systems for Repair and Strengthening of Concrete Bridge Elements”, American Association of State Highway and Transportation Officials, Washington, D.C.
2. ACI 440.2R-02 (2002). “Design and Construction of Externally Bonded FRP Systems for Strengthening Concrete Structures”, American Concrete Institute, Farmington Hills, MI.
3. ACI 440.2R-08 (2008). “Guide for the Design and Construction of Externally Bonded FRP Systems for Strengthening Concrete Structures”, American Concrete Institute, Farmington Hills, MI.
4. Al-Sulaimani, G. J., Istem, A., Basunbul, A. S., Baluch, M. H., and Ghaleb, B. N. (1994). “Shear repair for reinforced concrete by fiberglass plate bonding”, ACI Struct. J., 91 (3), 458–464.
5. Antoniades, K.K., Salonikios, T.N. and Kappos A.J. (2005). “Tests on Seismically Damaged Reinforced Concrete Walls Repaired and Strengthened Using Fiber-Reinforced Polymers”, ASCE, Journal of Composites for Construction, 9 (3), 236–246.
6. Arduini, M. and Nanni, A. (1997). “Behaviour of precracked RC beams strengthened with carbon FRP sheets”, Journal of Composites for Construction (ASCE), 1(2), 63-70.
7. Assih, T., Li, Y. and Delmas, Y. (1997). “Repairing of reinforced concrete beams by bonded carbon fiber composite sheets”, Proceedings of the US-Europe Workshop on Recent Advances in Bridge Engineering, Dubendorf, Switzerland, 119-126.
8. Bakis, C.E., Bank L.C., Brown V.L., Cosenza E., Davalos J.F., Lesko J.J., Machida A., Rizkalla S.H and Triantafillou, T.C. (2002), “Fiber-Reinforced Polymer Composites for Construction—State of-the-Art Review”, ASCE, Journal of Composites for Construction, 6 (2), 73–87.
9. Bank, L.C., Borowicz, D.T., Lamanna, A.J., Ray, J.C., and Velazquez, G.I. (2002). “Rapid Strengthening of Full-Size Reinforced Concrete Beams with Powder-Actuated Fastening Systems and Fiber-Reinforced Polymer (FRP) Composite Materials”, US Army Corps of Engineers, Report Number ERDC/GSL TR-02-12.
10. Barton, R. (1997). “Carbon fibre "plate bonding"”, Structural Survey, 15 (1), 11-14.
11. Blaschko, M., and Zilch, K. (1999). “Rehabilitation of concrete structures with strips glued into slits.” Proc., 12th Int. Conf. on Composite Materials (CD-ROM).
12. Borowicz, D.T. (2002). “Rapid strengthening of concrete beams with powder-actuated fastening systems and fiber reinforced polymer (FRP) composite materials”, MS thesis, Dept. of Civil Engineering, Univ. of Wisconsin-Madison, Madison, Wis.
13. Buyukozturk, O. and Hearing, B. (1998). “Failure behaviour of precracked concrete beams retrofitted with FRP”, J Compos Construct, 2 (3), 138-144.
14. CAN/CSA S806-02 (2002). “Design and construction of building structures with fibre-reinforced polymers”.

15. Canadian Standards Association (2004). “Design of concrete structures”, CSA A23.3-04, Rexdale, Ont.

16. Canadian Standards Association (2006) “Canadian highway bridge design code (CHBDC)”, CSA S6-06, Rexdale, Ont.

17. CECS-146 (2003). “Technical Specification for Strengthening Concrete Structures with Carbon Fiber Reinforced Polymer Laminates”, Code of Federal Regulations (CFR).

18. Ceroni, F., Pecce, M., Matthys, S. and Taerwe, L. (2007). “Debonding strength and anchorage devices for reinforced concrete elements strengthened with FRP sheets”, Elsevier J. Ltd., Composites: Part B, 429–441

19. Chaallal, O., Mofidi, A., Benmokrane B. and Neale, K. (2011) “Embedded Through-Section FRP Rod Method for Shear Strengthening of RC Beams: Performance and Comparison with Existing Techniques”, ASCE, Journal of Composites for Construction, 15 (3), 374–383.

20. Chajes, M. J., Januszka, T. F., Mertz, D. R., Thomson, T. A., and Finch, W. W. (1995). “Shear strength of RC beams using external applied composite fabrics”, ACI Struct. J., 92 (3), 295–303.

21. CNR-DT 200 (2004). “Guide for the Design and Construction of Externally Bonded FRP Systems for Strengthening Existing Structures”, Italian National Research Council, Rome, Italy.

22. Elarbi, A. (2011). “Durability Performance Of Frp Strengthened Concrete Beams And Columns Exposed To Hygrothermal Environment”, PhD Dissertation, Department of Civil and Environmental Engineering, Wayne State University, Detroit, MI.

23. Elarbi, A.M. and Wu, H.C. (2012). “Durability performance of epoxy exposed to different hygrothermal environments”, International SAMPE Technical Conference, North Charleston, SC, United States, 17p.

24. El-Hacha, R. and Rizkalla, S.H. (2004). “Near-surface-mounted fiber-reinforced polymer reinforcements for flexural strengthening of concrete structures”, ACI Structural Journal, 101 (5), 717-726.

25. El-Sokkary, H. and Galal, K. (2013). “Seismic Behavior of RC Shear Walls Strengthened with Fiber-Reinforced Polymer”, ASCE, Journal of Composites for Construction, 17 (5), 603-613.

26. El-Sokkary, H., Galal, K., Ghorbanirenani, I., Léger, P. and Tremblay, R. (2013). “Shake table tests on FRP-rehabilitated RC shear walls.” J. Compos. Constr., 17(1), 1–12.

27. Gaafar, M.A. and El-Hacha, R. (2008). “Strengthening reinforced concrete beams with prestressed near surface mounted FRP strips”, 4th International Conference on FRP Composites in Civil Engineering (CICE2008), Zurich, Switzerland.

28. Galal, K., Arafa, A. and Ghobarah, A. (2005). “Retrofit of RC square short columns”, Elsevier Ltd., Engineering Structures 27, 801–813.

29. Galal, K., and Mofidi, A. (2009). “Strengthening RC beams in flexure using new hybrid FRP sheet / ductile anchor system”, Journal of Composites for Construction, ASCE, 13 (3), 217-225.

30. Galal, K. and Mofidi, A. (2010). “Shear Strengthening of RC T-Beams Using Mechanically Anchored Unbonded Dry Carbon Fiber Sheets”, ASCE, Journal of Performance of Constructed Facilities, 24 (1), 31–39.

31. Galal, K., Seif ElDin, H.M. and Tirca, L. (2012) “Flexural Performance of Steel Girders Retrofitted Using CFRP Materials”, ASCE, Journal of Composites for Construction, 16 (3), 265–276.

32. Galal, K. and Sekar, M. (2007). “Rehabilitation of RC inverted-T girders using anchored CFRP sheets”, Elsevier Ltd., Composites: Part B 39, 604–617.

33. Ghobarah, A. and Galal, K. (2004) “Seismic rehabilitation of short rectangular RC columns”, Journal of Earthquake Engineering, 8 (1), 45–68.

34. Ghobarah, A. and Said, A. (2002) “Shear strengthening of beam–column joints”, Engineering Structures, 24 (7), 881–8.

35. Ghorbanirenani, I., Tremblay, R., Léger, P. and Leclerc, M. (2012). “Shake table testing of slender RC shear walls subjected to eastern North America seismic ground motions”, J. Struct. Eng., 138(12), 1515–1529.

36. Gillespie, J. W., Jr., Mertz, D. R., Kasai, K., Edberg, W. M., Demitz, J. R., and Hodgson, I. (1996). “Rehabilitation of steel bridge girders: Large scale testing”, Proc. of the 11th Technical Conf. of the American Society for Composites, Technomic, Lancaster, PA, 231–240.

37. Hall J.D., Schuman H.R. and Hamilton H. (2002). “Ductile anchorage for connecting FRP strengthening of under reinforced masonry building”, ASCE J. Compos. Construction, 6 (1).

38. Hollaway, L. C. and Garden, H. N. (1998). “An experimental study of the failure modes of reinforced concrete beams strengthened with pre- stressed carbon composite plates”, Composites, Part B, 29 (4), 411– 424.

39. ISIS Canada (2008). “Design manual No.4: FRP Rehabilitation of Reinforced Concrete Structures”**,** Canadian Network of Centers of Excellence on Intelligent Sensing for Innovative Structure, Canada.

40. ISIS Canada Educational Module No. 4 (2006). “An Introduction to FRP-Strengthening of Concrete Structures”, Canadian Network of Centers of Excellence on Intelligent Sensing for Innovative Structure, Canada.

41. JSCE (2001). “Recommendations for Upgrading of Concrete Structures with Use of Continuous Fiber Sheets”, Japan Society of Civil Engineers, Tokyo, Japan.

42. Jung, W., Park, J. and Park, Y. (2007). “A Study on the flexural behaviour of reinforced concrete beams strengthened with NSM prestressed CFRP reinforcement”, Proceeding of the 8th International Symposium on Fiber Reinforced Polymer Reinforcement for Reinforced Concrete Structures (FRPRCS-8), University of Patras, Patras, Greece, (CD-ROM, 8p).

43. Karantzikis M., Papanicolaou C.G., Antonopoupos C.P. andTriantafillou T.C. (2005). “Experimental investigation of nonconventional confinement for concrete using FRP”, J. Compos. Constr., ASCE, 9(6), 480–7.

44. Karbhari, V.M. (2004). “E-glass/Vinylester composite in aqueous environments: effects on short-beam shear strength”, Journal of Composites for Construction, ASCE, 8 (2), 148-156.

45. Karbhari, V. and Howie, I. (1997). “Effect of Composite Wrap Architecture on Strengthening of Concrete Due to Confinement: II-Strain and Damage Effects”, Journal of Reinforced Plastics and Composites, 16 (2), 1039-1063.

46. Koayshi, K., Fujii, S., Yabe, Y., Tukagoshi, H. and Sugiyama, T. (2001). “Advanced wrapping system with CF-anchor: Stress Transfer mechanism of CF anchor”, Proceedings of FRPRCS5 International symposium, Cambridge, UK.

47. Khalifa, A., Alkhrdaji, T., Nanni, A., and Lansburg, S. (1999). “Anchorage of surface mounted FRP reinforcement”, Concr. Int.: Des. Constr., 21 (10), 49–54.

48. Lane J.S., Leeming M.B. and Fashole-Luke P.S. (1997). “Using advanced composite materials in bridge strengthening: Introduction project ROBUST”, Structural Engineering Journal, 75 (1), 16.

49. Lees, J. M., Winistörfer, A. U., and Meier, U. (2002). “External prestressed carbon fiber reinforced polymer straps for shear enhancement of concrete”, J. Compos. Constr., 6(4), 249–256.

50. Liu, X., Silva, P. R., and Nanni, A. (2001). “Rehabilitation of steel bridge members with FRP composite materials”, Proc., CCC 2001, Composites in Construction, Porto, Portugal, 613–617.

51. Lorenzis, L.D. (2001). “A comparative study of models on confinement of concrete cylinders with FRP composites”, Research report, Chalmers University of Technology, Goteborg, Sweden.

52. Maalej, M. and Bonacci, J.F. (1998). “Repair and strengthening of beams using FRP reinforcement”, Proceedings of the 1998 Annual Conference of the Canadian Society for Civil Engineering. Halifax, Nova Scotia, Vol. IIIb: 643-652.

53. Manos, G. C., Katakalos, K., Kourtides, V., and Mitsarakis, C. (2007). “Upgrading the flexural capacity of a vertical R/C member using carbon fiber reinforcing plastics applied externally and anchored at the foundation.” Proc., AFRPRCS-8 Symp. 2007 (CD-ROM).

54. Meier, U. (1992). “Carbon Fiber-Reinforced Polymers: Modern Materials in Bridge Engineering”, Structural Engineering International, 2 (1), 7-12.

55. Meier, U. (1995). “Strengthening of structures using carbon fiber/epoxy composites”, Construct Building Mat, 9 (6), 341-351.

56. Meier, U. and Kaiser, H. (1991). “Strengthening of Structures with CFRP Laminates”, Advanced Composite Materials in Civil Engineering Structures, ASCE Specialty Conference, 224-232.

57. Nagy-Gyorgy T., Mosoarca M., Stoian V., Gergely J. and Dan D. (2005). “Retrofit of reinforced concrete shear walls with CFRP composites”, Proceedings of fib Symposium ‘‘Keep concrete Attractive’’, Budapest, Hungary, 897–902.

58. NCHRP Report 678 (2011). “Design of FRP Systems for Strengthening Concrete Girders in Shear”, Washington, D.C.

59. Nordin, H. (2003). “Flexural strengthening of concrete structures with prestressed near surface mounted CFRP rods”, PhD Thesis, Department of Civil and Mining Engineering, Division of Structural Engineering, LULEÅ University of Technology.

60. Patnaik, A., Bauer, C., and Srivatsan, T. (2008). “The extrinsic influence of carbon fibre reinforced plastic laminates to strengthen steel structures.” Sadhana, 33(3), 261–272.

61. Pesic, N. and Pilakoutas, K (2003). “Concrete beams with externally bonded flexural FRP-reinforcement: analytical investigation of debonding failure”, Composites Part B: Engineering, 34 (4).

62. Quattlebaum, J. B., Harries, K. A. and Petrou, M. F. (2005). “Comparison of three flexural retrofit systems under monotonic and fatigue loads.” J. Bridge Eng., 10 (6), 731–740.

63. Ritchie, P., Thomas, D., Lu, L. and Conneley, G. (1991). “External Reinforcement of Concrete Beams Using Fiber Reinforced Plastics”, ACI Structural Journal, 88 (4), 490-500.

64. Rizkalla S., Dawood M. and Schnerch D. (2008), “Development of a carbon fiber reinforced polymer system for strengthening steel structures.”, Elsevier J. Ltd., Composites: Part A 39, 388–397

65. Saadatmanesh, E. and Ehsani, M. R. (1989). “Application of fibre composites in civil engineering” Proc., 7th ASCE Structures Congress, ASCE, New York, 526–535.

66. Sharif, A., Al-Sulaimani, G., Basunbul, I., Baluch, M. and Ghaleb, B. (1994). “Strengthening of Initially Loaded Reinforced Concrete Beams Using FRP Plates”, ACI Structural Journal, 91 (2), 160-168.

67. Sika Corporation (1999), “Sika Carbodur Structural Strengthening System – Engineering Guidelines for Design and Application”, Sika Corporation.

68. Sika Corporation (2014), “Refurbishment Structural Strengthening with Sika Systems”, Sika Corporation.

69. Tan, K.H. and Mathivoli, M. (1999). “Behavior of preloaded reinforced concrete beams strengthened with carbon fiber sheets”. Proceedings of the 4th International Symposium on Fiber Reinforced Polymer Reinforcement for Reinforced Concrete Structures, (FRPRCS-4). Baltimore, 159-170

70. Thomsen, H., Spacone, E., Limkatanyu, S. and Camata, G. (2004), “Failure Mode Analyses of Reinforced Concrete Beams Strengthened in Flexure with Externally Bonded Fiber-Reinforced Polymers”, Journal of Composites for Construction, 8, 123–131.

71. TR-55 (2000). “Design Guidance for Strengthening Concrete Structures Using Fiber Composite Materials”, The Concrete Society (TCS), Berkshire, United Kingdom.

72. Triantafillou, T. C. (1998). “Shear strengthening of reinforced concrete beams using epoxy bonded FRP composites.” ACI Struct. J., 95 (2), 107–115.

73. USDOT, FHWA (2010). “2010 Status of the Nation's Highways, Bridges, and Transit: Conditions and Performance”, Federal Highway Administration, Washington, D.C.

74. Velázquez, G.I., Ray, J.C., Borowicz, D.T., Lamanna, A.J., Arora D. and Bank, L.C. (2002). “Tests of Reinforced Concrete T-Beams Retrofitted with Mechanically Anchored Fiber-

Reinforced Polymer (FRP) Plates", 1st International Conference on Bridge Maintenance, Safety and Management, IABMAS, Barcelona, SPAIN, (CD-ROM).

75. Winistorfer, A. U. (1999). "Development of non-laminated advanced composite straps for civil engineering applications", PhD thesis, Univ. of Warwick, U.K.
76. Wu, H.C., Fu, G., Gibson, R.F., Warnemuende, K., Yan, A. and Anumandla, V. (2006). "Durability testing of FRP material in low temperature weathering condition", in CD Proc. 21st Annual Technical Conference, American Society of Composites, Dearborn, MI.
77. Wu, H.C., Fu, G., Gibson, R.F., Yan, A., Warnemuende, K. and Anumandla, V. (2006) "Durability of FRP Composite Bridge Deck Materials under Freeze-Thaw and Low Temperature Conditions." Journal of Bridge Engineering, 11 (4), 443-451.

**Bibliography:**

1. Bank, L.C., Oliva, M.G., Arora, D. and Borowicz, D.T. (2003). "Rapid Strengthening of Reinforced Concrete Bridges", University of Wisconsin – Madison, Department of Civil and Environmental Engineering, Wisconsin Department of Transportation, p.166.
2. Eamon, C. D., Wu, H.C., Makkawy, A.A. and Siavashi, S. (2014). "Design and Construction Guidelines for Strengthening Bridges using Fiber Reinforced Polymers (FRP)", Wayne State University, Michigan Department of Transportation, p.368.
3. El-Hacha, R., Wight, R.G. and Green M.F (2001). "Prestressed fibre-reinforced polymer laminates for strengthening structures", Prog. Struct. Engng Mater, 3, 111-121.
4. Park, S.H., Robertson, I.N. and Riggs, H.R. (2002), "A Primer for FRP Strengthening of Structurally Deficient Bridges", State of Hawaii: Department of Transportation: Highway Division, FHWA (Federal Highway Administration), University of Hawaii at Manoa, p.76.
5. Setunge, S., Kumar. A., Nazemian, A., De Silva, S., Carse, A., Spathonis, J., Chandler, L., Gilbert, D., Johnson, B., Jeary, A., Pham, L. (2002). "User Friendly Guide for Rehabilitation or Strengthening of Bridge Structures Using Fiber Reinforced Polymer Composites", CRC Construction Innovation, Australia.